

Considerations for selection of a mass spectrometer to measure sulfur isotopes at Io

- Environmental models
 - Partitioning between particulates, neutrals, and ions (ion-neutral chemistry)
 - Differences in loss processes (thermal escape, plume eruptions, ion pickup)
- Reactivity of compounds on mass spectrometer surfaces (open versus closed source)
- Required resolution ($^{34}\text{S}^{16}\text{O}_2$ versus $^{32}\text{S}^{18}\text{O}^{16}\text{O}$ requires $\sim 8000 M/\Delta M$ at 10% peak valley with the approximate abundance difference is 22.)
- Required sensitivity (abundance of SO_2 , SO , etc.)
- Mission resources available (mass, power, and cost available in the mission)

Table 19.2. Summary of Io atmospheric species.

Species	Io Abundance*	Reference
SO ₂	$\sim(1-10) \times 10^{16}$ in $\sim \pm(30-45)^\circ$ latitude band $\sim(2-10?) \times$ higher in active volcanoes	Synthesis of all observations; see Sections 19.2.2, 19.2.3, and 19.2.4; McGrath <i>et al.</i> 2000a; Spencer <i>et al.</i> 2000; Spencer <i>et al.</i> 2002; Jessup <i>et al.</i> 2004
S ₂	1×10^{16} , Pele plume (t), SO ₂ /S ₂ $\sim(3-12)$	Spencer <i>et al.</i> 2000
SO	$\sim(0.03-0.1) \times$ SO ₂	Lellouch 1996
NaCl	$(0.003-0.013) \times$ SO ₂ , active volcanoes	Lellouch <i>et al.</i> 2003
O ₂	Inferred (modeling)	Kumar (1982, 1985); Summers 1985; Summers and Strobel 1996; Wong and Johnson 1995, 1996; Wong and Smyth 2000; Moses <i>et al.</i> 2002a, 2002b
S	$3.6 \times 10^{12} < \mathcal{N}_S < 1.3 \times 10^{14}$ (t) $\sim 9 \times 10^{12}$ at $2 R_{Io}$ (t) = $0.1 \times$ O	Feaga <i>et al.</i> 2002 (upper limit revised up; see text) Wolven <i>et al.</i> 2001
O	$>(4-7) \times 10^{13}$, disk average $\sim 1 \times 10^{14}$ at $2 R_{Io}$ (t) = $11 \times$ S	Ballester 1989 Wolven <i>et al.</i> 2001
Na	4×10^{12} , disk average	Bouchez <i>et al.</i> 2000 [see also Burger <i>et al.</i> 2001, Retherford 2002]
K	$(1-10) \times 10^8$; Na/K = 10 ± 5 at $(10-20) R_{Io}$	Brown 2001
Cl	$\sim 1 \times 10^{13}$, disk average	Feaga <i>et al.</i> (2004)
H	$\sim 2 \times 10^{12}$	Strobel and Wolven 2001
CS ₂	$< 2 \times 10^{14}$	McGrath <i>et al.</i> 2000a; Spencer <i>et al.</i> 2000; Spencer <i>et al.</i> 2002
CO	$< (3.6-6) \times 10^{17}$	Lellouch <i>et al.</i> 1992
H ₂ S	$< (0.7-1.2) \times 10^{16}$	Lellouch <i>et al.</i> 1992
OCS, S ₂ O, ClO, CS, NaOH	Not detected (mm)	Lellouch <i>et al.</i> 1992
KCl	$< 1 \times$ NaCl	Lellouch <i>et al.</i> 2003

* Numbers in vertical column density, cm⁻², unless otherwise noted; (t) = tangential.

Melissa A. McGrath
Space Telescope Science Institute

Emmanuel Lellouch
Observatoire de Paris

Darrell F. Strobel, Paul D. Feldman
The Johns Hopkins University

Robert E. Johnson
University of Virginia

Io Photochemistry

PHOTOCHEMISTRY AND TRANSPORT IN IO'S ATMOSPHERE

TABLE I
Selected Photochemical Reactions

Reaction	Rate Coefficient ^{a,b}	Comments
R1a $SO_2 + h\nu \rightarrow SO + O$	1.0(-5)	Okabe(1971), Welge (1974)
b $\rightarrow S + O_2$	6.3(-7)	Driscoll & Warneck (1968)
R2 $SO + h\nu \rightarrow S + O$	1.8(-5)	Phillips (1981)
R3a $O_2 + h\nu \rightarrow O + O$	3.9(-10)	Hudson (1971)
b $\rightarrow O(^1D) + O$	9.4(-8)	
R4 $S_2 + h\nu \rightarrow S + S$	9.2(-5)	Brewer & Brabson (1986)
R5 $Na_2 + h\nu \rightarrow Na + Na$	3.0(-4)	see text
R6a $NaO_2 + h\nu \rightarrow NaO + O$	9.0(-5)	Plane (1991)
b $\rightarrow Na + O_2$	1.0(-5)	0.1 branching assumed
R7a $NaS_2 + h\nu \rightarrow NaS + S$	9.0(-5)	like $NaO_2 + h\nu$
b $\rightarrow Na + S_2$	1.0(-5)	0.1 branching assumed
R8 $Na_2O + h\nu \rightarrow NaO + Na$	1.0(-5)	assumed
R9 $Na_2S + h\nu \rightarrow NaS + Na$	1.0(-5)	assumed
R10 $S + O_2 \rightarrow SO + O$	2.3(-12)	JPL92
R11 $SO + SO \rightarrow SO_2 + S$	5.8(-12)e ^{-1760/T}	HH92
R12 $SO + O_2 \rightarrow SO_2 + O$	2.6(-13)e ^{-2400/T}	JPL92
R13 $O + S_2 \rightarrow S + O_2$	2.2(-11)e ^{-84/T}	Yung & DeMore (1982)
R14 $SO + SO_3 \rightarrow 2SO_2$	2.5(-15)	Yung & DeMore (1982)
R15 $O + O + M \rightarrow O_2 + M$	1.0(-26)T ^{-2.9}	NIST (1994)
R16 $SO + O + M \rightarrow SO_2 + M$	7.7(-31)	Yung & DeMore (1982)
R17 $SO_2 + O + M \rightarrow SO_3 + M$	3.4(-32)e ^{-1120/T}	Yung & DeMore (1982)
R18 $S + S + M \rightarrow S_2 + M$	1.0(-26)T ^{-2.9}	Baulch & Drysdale (1973)
R19 $NaO + O \rightarrow Na + O_2$	3.7(-10)	JPL92
R20 $NaO_2 + O \rightarrow NaO + O_2$	5.0(-13)	Plane (1991)
R21a $Na_2O + O \rightarrow 2NaO$	1.0(-12)	assumed
b $\rightarrow Na_2 + O_2$	$\phi_{Na_2} k_{19a}$	
R22a $Na_2O + S \rightarrow NaO + NaS$	1.0(-12)	assumed
b $\rightarrow Na_2 + SO$	$\phi_{Na_2} k_{20a}$	
R23 $Na + O + M \rightarrow NaO + M$	1.0(-33)	assumed
R24 $Na + O_2 + M \rightarrow NaO_2 + M$	2.2(-27)T ^{-1.2}	JPL92
R25 $NaO + O_2 + M \rightarrow NaO_3 + M$	3.1(-25)T ^{-2.0}	JPL92
R26 $NaS + O \rightarrow Na + SO$	3.7(-10)	like $NaO + O$
R27 $NaS_2 + O \rightarrow NaS + SO$	5.0(-13)	like $NaO_2 + O_2$
R28a $Na_2S + O \rightarrow NaS + NaO$	1.0(-12)	assumed
b $\rightarrow Na_2 + SO$	$\phi_{Na_2} k_{26a}$	
R29a $Na_2S + S \rightarrow 2NaS$	1.0(-12)	assumed
b $\rightarrow Na_2 + S_2$	$\phi_{Na_2} k_{27a}$	
R30 $Na_2 + O \rightarrow NaO + Na$	5.0(-10)	assumed
R31 $Na_2 + S \rightarrow NaS + Na$	5.0(-10)	assumed

^a Photodissociation coefficients for zero optical depth, hemispheric average, with units of sec⁻¹. Bimolecular and termolecular rate coefficients have units cm³ sec⁻¹, and cm⁶ sec⁻¹, respectively.

^b A(-B) is read A × 10^{-B}.

ICARUS 120, 290-316 (1996)
ARTICLE NO. 0051

Photochemistry and Vertical Transport in Io's Atmosphere and Ionosphere

MICHAEL E. SUMMERS

E. O. Hulbert Center for Space Research, Naval Research Laboratory, Washington, DC 20375
E-mail: summers@map.nrl.navy.mil

AND

DARRELL F. STROBEL

Department of Earth and Planetary Sciences, Center for Astrophysical Sciences, and Department of Physics and Astronomy, The Johns Hopkins University, Baltimore, Maryland 21218

Received May 19, 1995; revised October 2, 1995

PHOTOCHEMISTRY AND TRANSPORT IN IO'S ATMOSPHERE

TABLE II
Ionospheric Reactions

Reaction	Rate Coefficient ^{a,b}	Comments ^c
R32 $SO_2 + h\nu \rightarrow SO_2^+ + e$	4.2(-8)	Wu & Judge (1981)
R33 $O_2 + h\nu \rightarrow O_2^+ + e$	1.8(-8)	
R34 $SO + h\nu \rightarrow SO^+ + e$	1.8(-8)	
R35 $O + h\nu \rightarrow O^+ + e$	7.6(-9)	McGuire (1968)
R36 $S + h\nu \rightarrow S^+ + e$	7.6(-9)	"
R37 $Na + h\nu \rightarrow Na^+ + e$	3.6(-7)	"
R38 $O^+ + SO_2 \rightarrow O_2^+ + SO$	8.0(-10)	AH86
R39 $O^+ + SO \rightarrow SO^+ + O$	5.0(-10)	assumed
R40 $O^+ + O_2 \rightarrow O_2^+ + O$	1.1(-10)	A93
R41 $O^+ + S \rightarrow S^+ + O$	5.0(-10)	assumed
R42 $O^+ + Na \rightarrow Na^+ + O$	5.0(-10)	assumed
R43 $S^+ + SO \rightarrow SO^+ + S$	1.0(-9)	assumed
R44 $S^+ + O_2 \rightarrow SO^+ + O$	2.3(-11)	AH86
R45 $S^+ + Na \rightarrow Na^+ + S$	5.0(-10)	assumed
R46 $SO^+ + SO \rightarrow S^+ + SO_2$	1.0(-11)	assumed
R47 $SO^+ + Na \rightarrow Na^+ + SO$	5.0(-10)	assumed
R48 $O_2^+ + S \rightarrow S^+ + O_2$	5.0(-10)	assumed
R49 $O_2^+ + SO \rightarrow SO^+ + O_2$	1.0(-10)	assumed
R50a $O_2^+ + Na \rightarrow Na^+ + O_2$	6.3(-10)	AH86
b $\rightarrow NaO^+ + O$	7.1(-11)	
R51a $SO_2^+ + S \rightarrow SO^+ + O_2$	5.0(-10)	assumed
b $\rightarrow S^+ + SO_2$	1.0(-10)	
R52 $SO_2^+ + SO \rightarrow SO^+ + SO_2$	5.0(-10)	assumed
R53 $SO_2^+ + O \rightarrow SO^+ + O_2$	1.0(-10)	assumed
R54 $SO_2^+ + O_2 \rightarrow O_2^+ + SO_2$	2.5(-10)	AH86
R55a $SO_2^+ + Na \rightarrow Na^+ + SO_2$	5.0(-10)	assumed
b $\rightarrow NaO^+ + SO$	5.0(-10)	assumed
R56 $Na^+ + Na_2 \rightarrow Na_2^+ + Na$	5.0(-10)	assumed
R57 $Na^+ + Na_2O \rightarrow Na_2O^+ + Na$	1.0(-9)	assumed
R58 $Na^+ + Na_2S \rightarrow Na_2S^+ + Na$	1.0(-9)	assumed
R59 $Na^+ + e \rightarrow Na$	2.7(-12) ($\frac{3000}{T}$) ⁶⁹	PH80
R60 $NaO^+ + e \rightarrow Na + O$	2.0(-7) ($\frac{3000}{T}$) ⁵⁰	assumed
R61 $S^+ + e \rightarrow S$	3.9(-12) ($\frac{3000}{T}$) ⁶³	PH80
R62 $O^+ + e \rightarrow O$	3.9(-12) ($\frac{3000}{T}$) ⁶³	assumed
R63 $O_2^+ + e \rightarrow O + O$	2.0(-7) ($\frac{3000}{T}$) ⁵⁰	assumed
R64 $SO^+ + e \rightarrow S + O$	2.0(-7) ($\frac{3000}{T}$) ⁵⁰	assumed
R65 $SO_2^+ + e \rightarrow SO + O$	3.0(-7) ($\frac{3000}{T}$) ⁵⁰	assumed
R66 $Na_2^+ + e \rightarrow Na + Na$	3.0(-7) ($\frac{3000}{T}$) ⁵⁰	assumed
R67 $Na_2O^+ + e \rightarrow NaO + Na$	2.0(-7) ($\frac{3000}{T}$) ⁵⁰	assumed
R68 $Na_2S^+ + e \rightarrow NaS + Na$	2.0(-7) ($\frac{3000}{T}$) ⁵⁰	assumed

^a Photoionization coefficients for zero optical depth, hemispheric average, with units of sec⁻¹. Ion-molecule rate coefficients have units cm³ sec⁻¹.

^b A(-B) is read A × 10^{-B}.

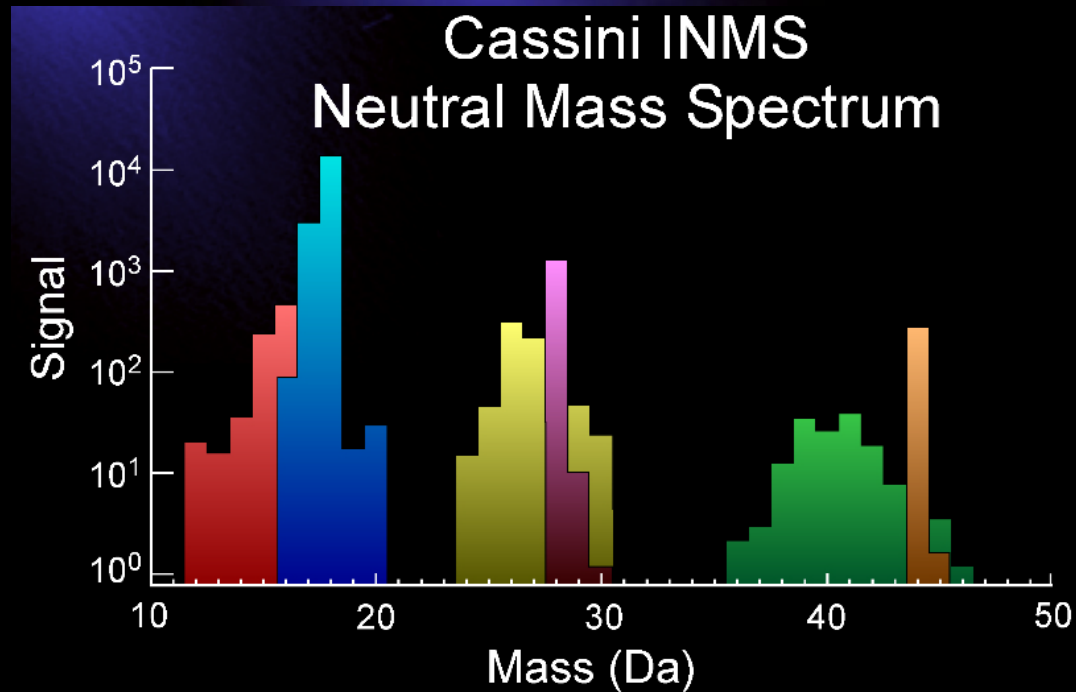
^c AH86 is Anicich and Huntress (1986), PH80 is Prasad and Huntress (1980), and A93 is Anicich (1993).

Sulfur Compounds are Reactive

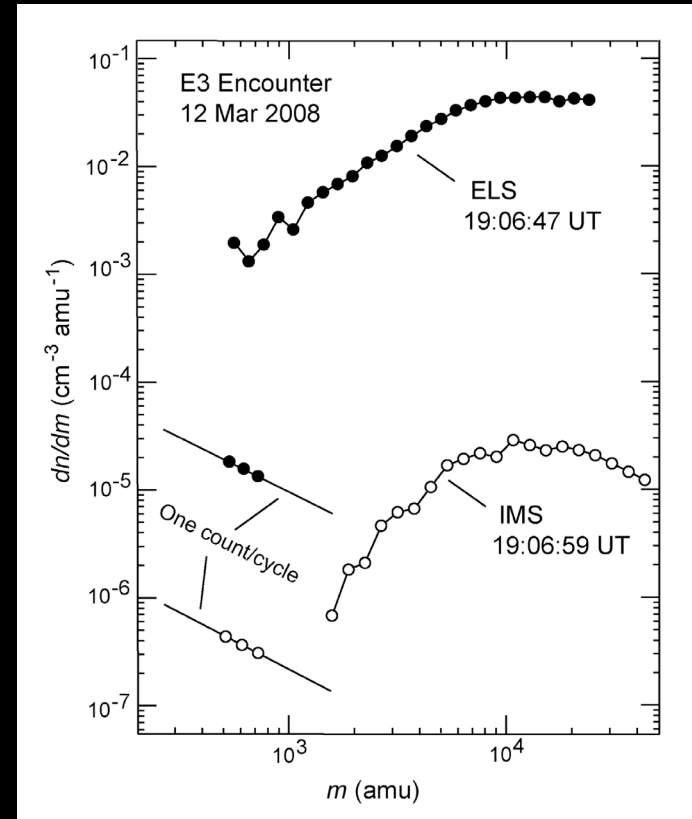
TO MEASURE IONS AND REACTIVE NEUTRALS AN OPEN SOURCE IS NEEDED

What lessons have we learned from Cassini?

Enceladus The Cryo-Geyser



Volatile composition like a comet?



Nano ice grains that contain water
cluster ions and carbonates?

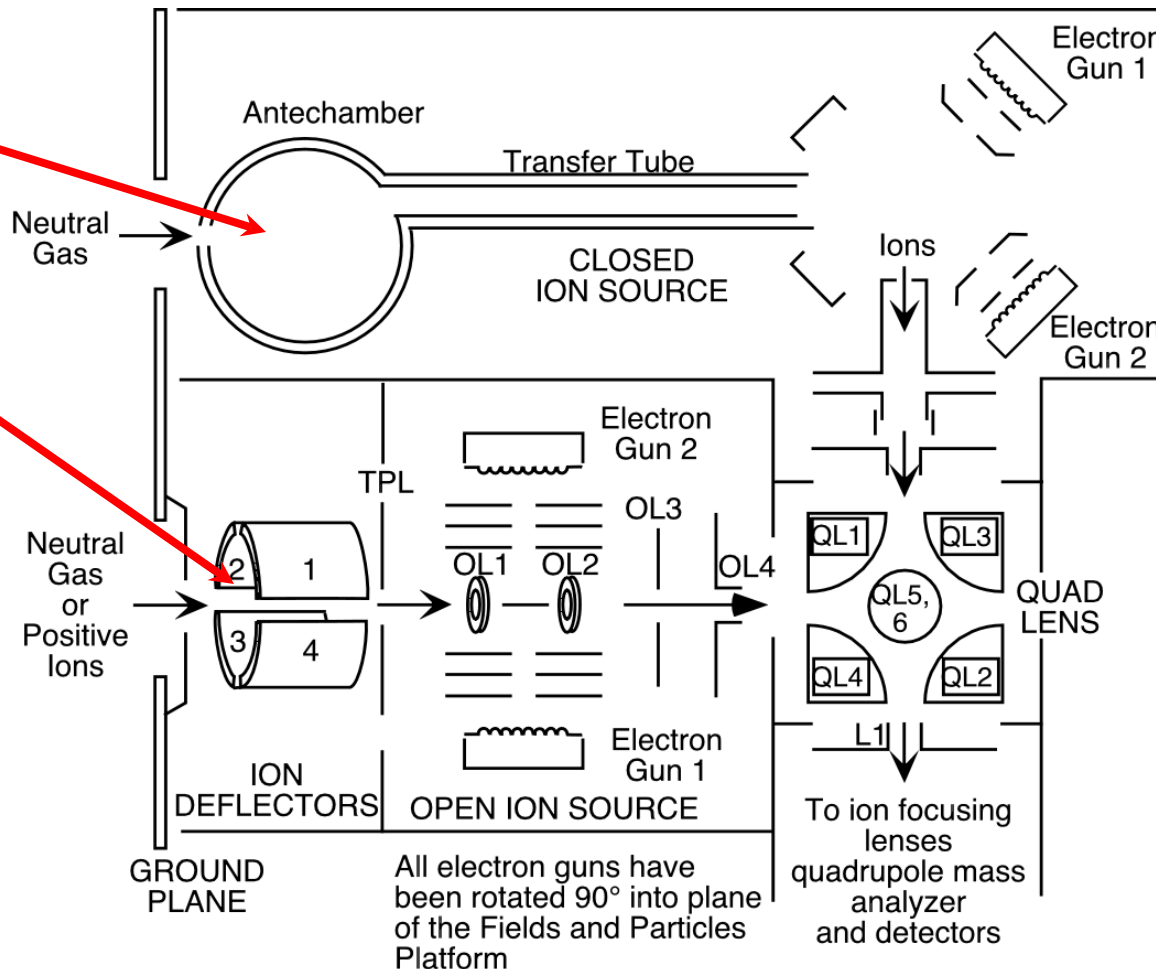
Ion Neutral Mass Spectrometer Instrument Configuration

During the Enceladus flybys:

- Neutral densities from closed source
- Ion densities from open source

Note: Dissociative ionization helps determine the mass deconvolution.

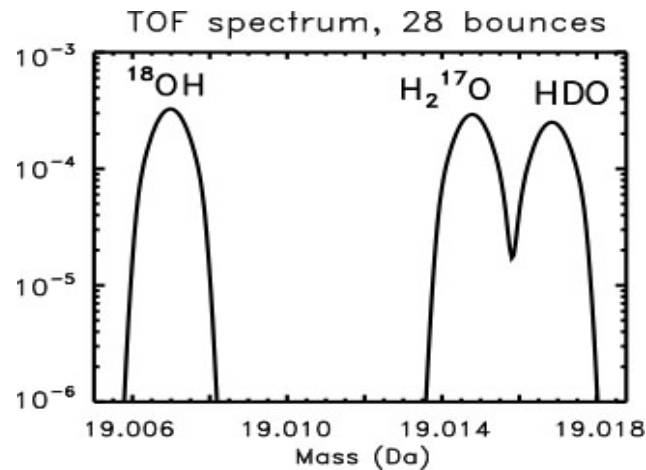
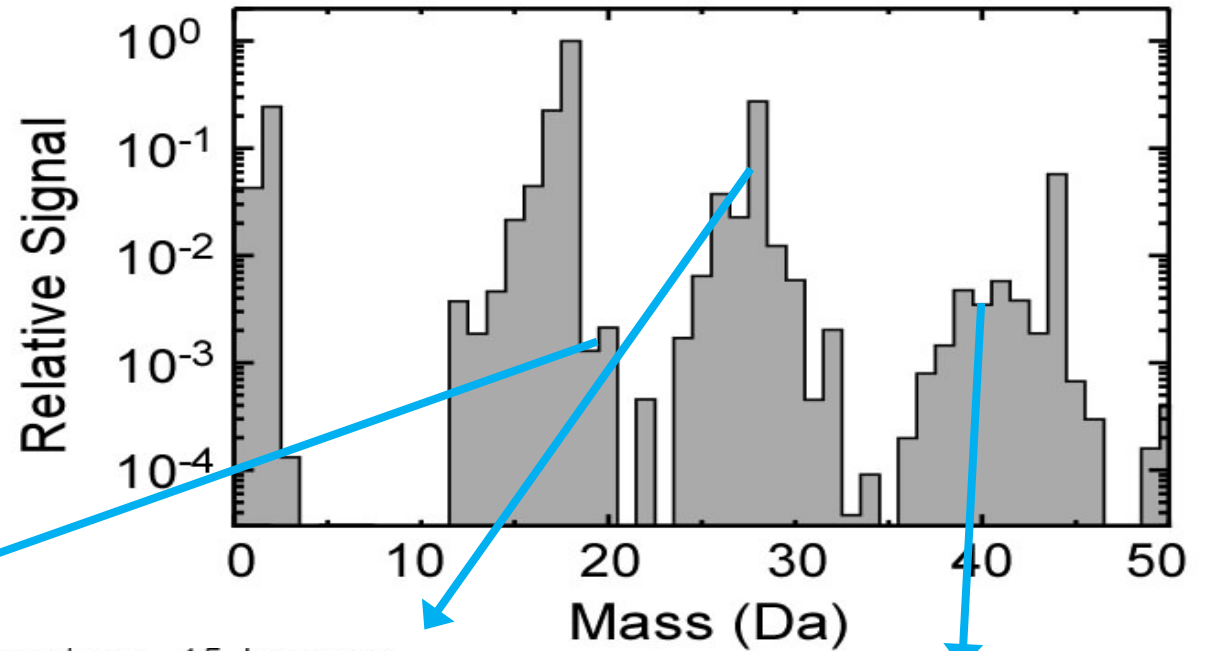
For example, a molecule of N_2 penetrating inside the closed source can be ionized and dissociated into N_2^+ and N^+ and be observed in the detector on mass channels 28 and 14.



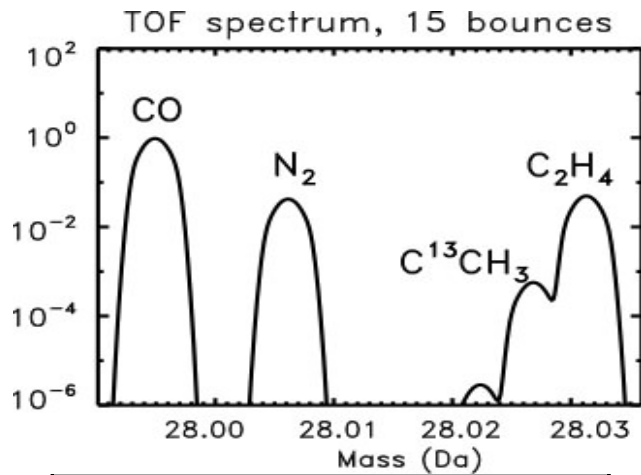
Decoding Enceladus with High Resolution MS

A dynamic range of $\sim 10^8$ and mass resolution on the order of 17,000 ($M/\Delta M$) at 1% peak height is necessary to settle the most important current questions about the composition of Enceladus' plume:

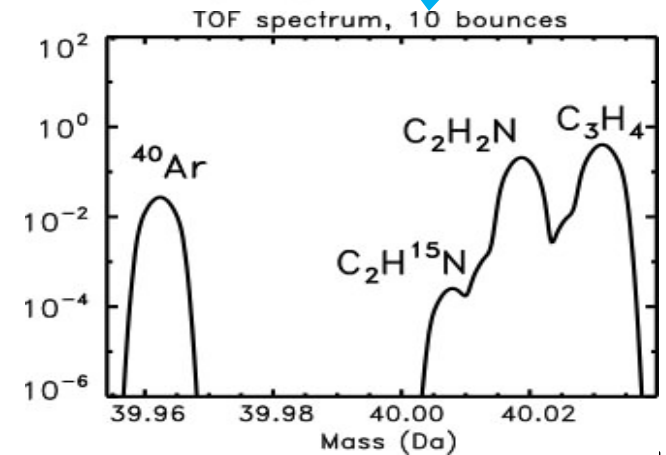
- direct measurement of all H₂O isotopes
- determine C, N, O content via numerous separations (N₂ vs. CO, HCN vs. C₂H₄, H₂CO vs. C₂H₆, etc.)
- determination of noble gases such as Ar



M=19
H₂O isotopes
~16,300 (28 bounces)



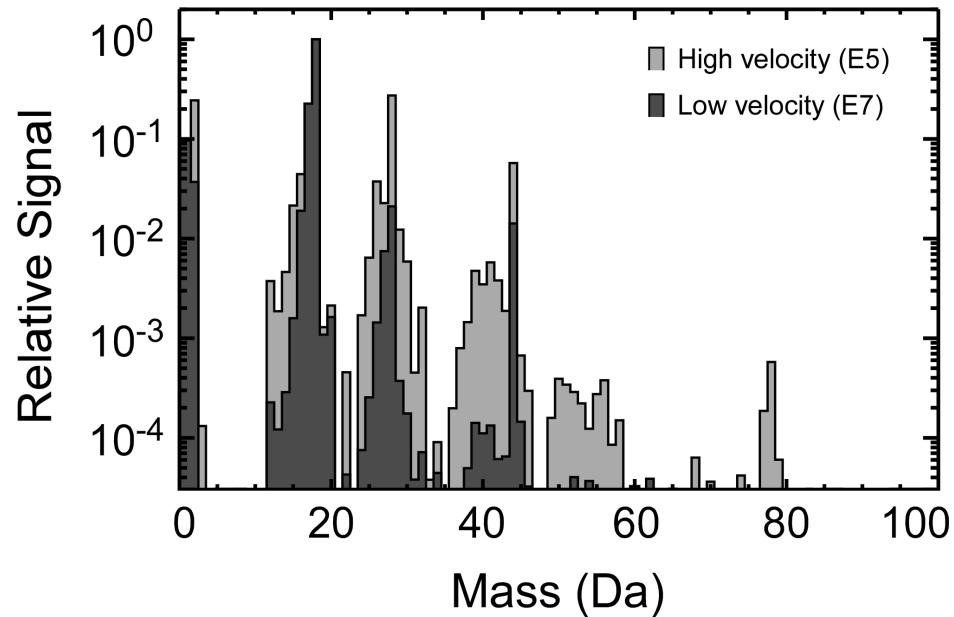
M=28
CO, N₂, C₂H₄
~10,900 (15 bounces)



M=40
C₃H₄, C₂H₂N, ⁴⁰Ar
~8,750 (10 bounces)

The Mass Spectra Vary with Flyby Velocity

- Mass Spectra



- Elemental Composition

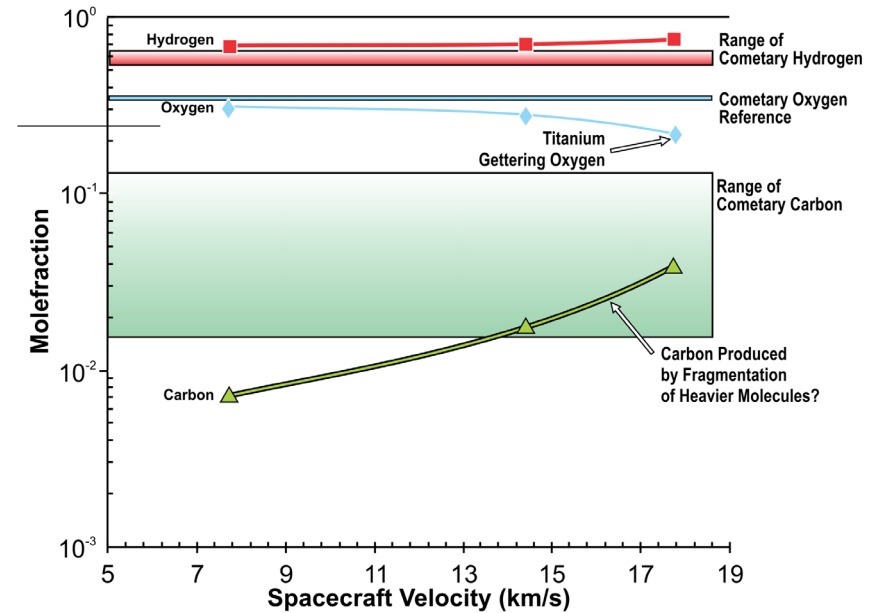
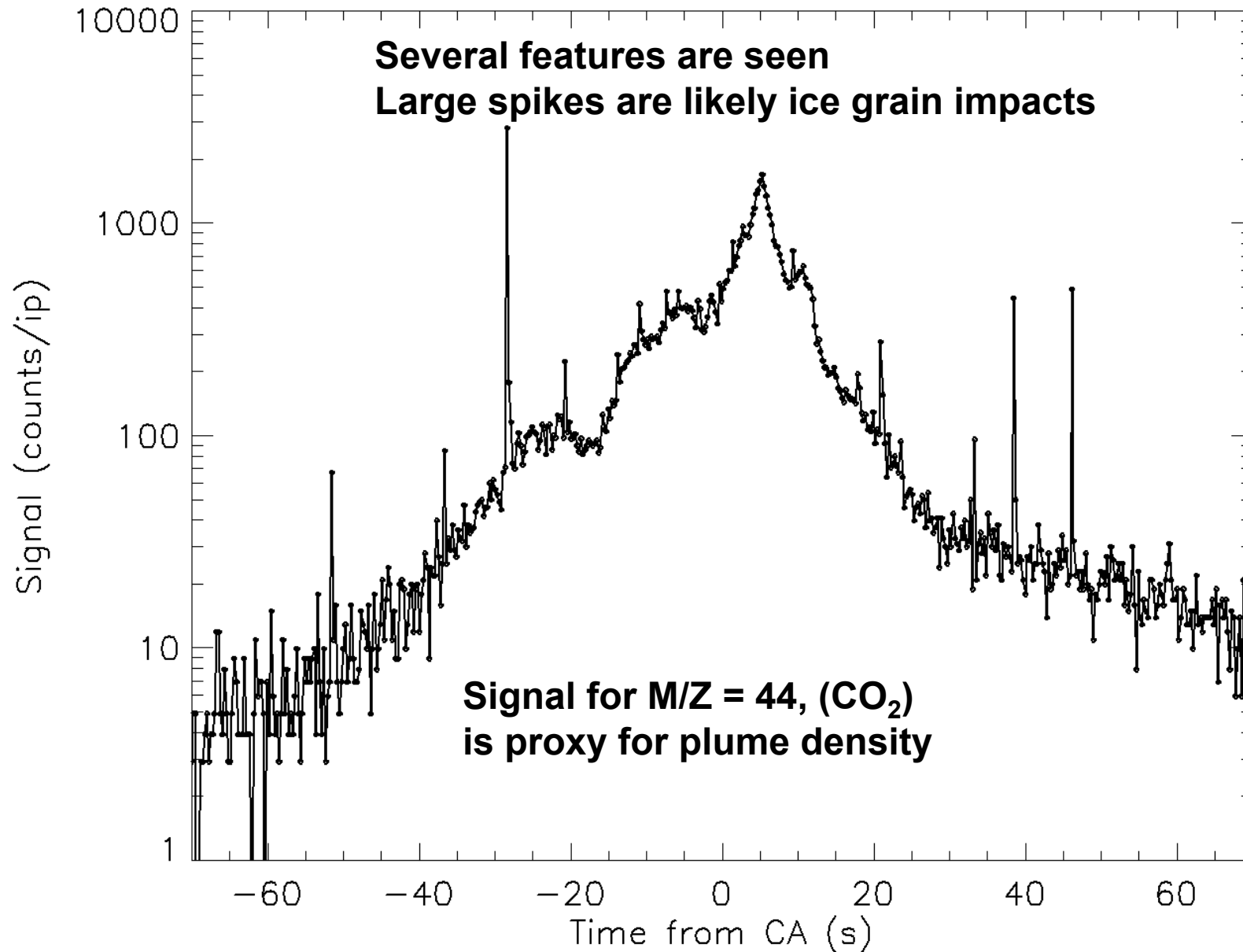


Figure 3: Element Abundances in Plume. Cometary composition taken from Bocklée-Morvan, Comets II, 2005.

Ta008538

Velocity varies from 7.7 km s^{-1} (E14, E17, E18) to 17.7 km s^{-1} (E5)

Plume Signal versus Time from Closest Approach



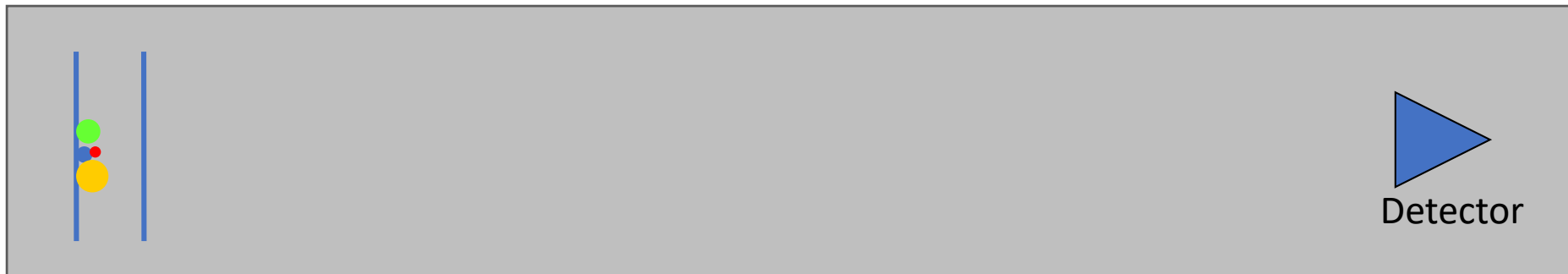
MASS SPECTROMETER OPTIONS

Consideration of mass resolution and sensitivity versus mass and power resources

How does Time of Flight (TOF) work?

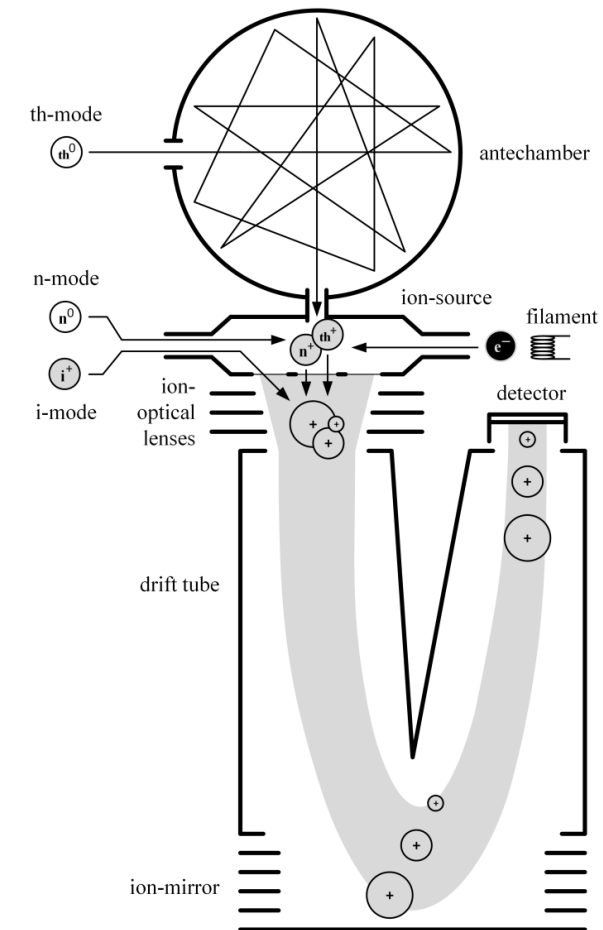
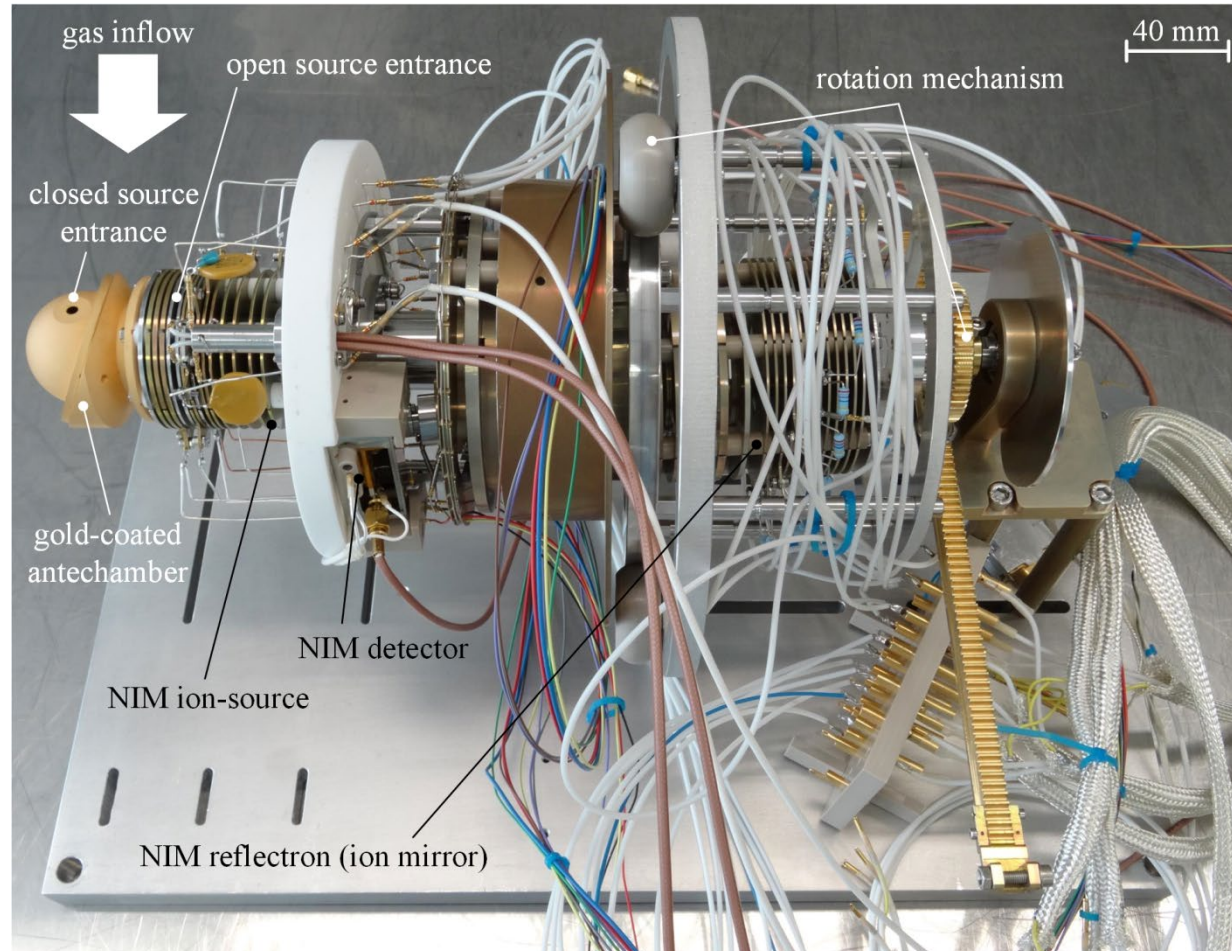
TOF Concept

- A packet of ions is accelerated to a defined kinetic energy and the time required to move through a fixed distance is measured
- As $KE = mv^2/2$ then lighter ions travel faster than heavier ones → mass separation
- The greater the distance between source and detector the smaller the mass difference that can be seen (resolution)

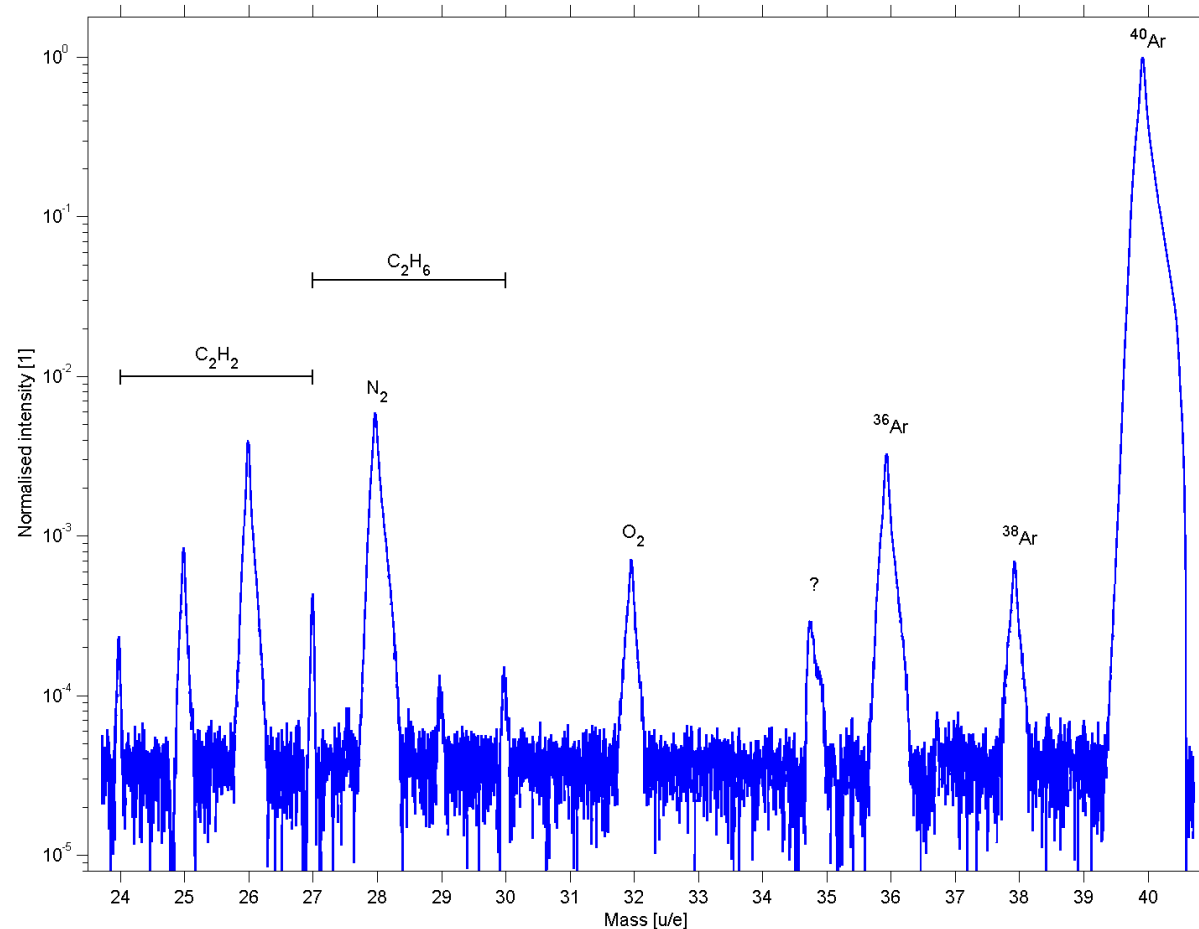




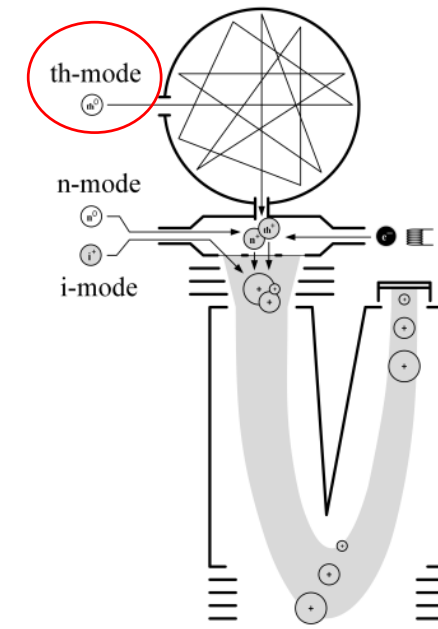
NIM/PEP/JUICE prototype



NIM /PEP /JUICE Prototype: Dynamic range

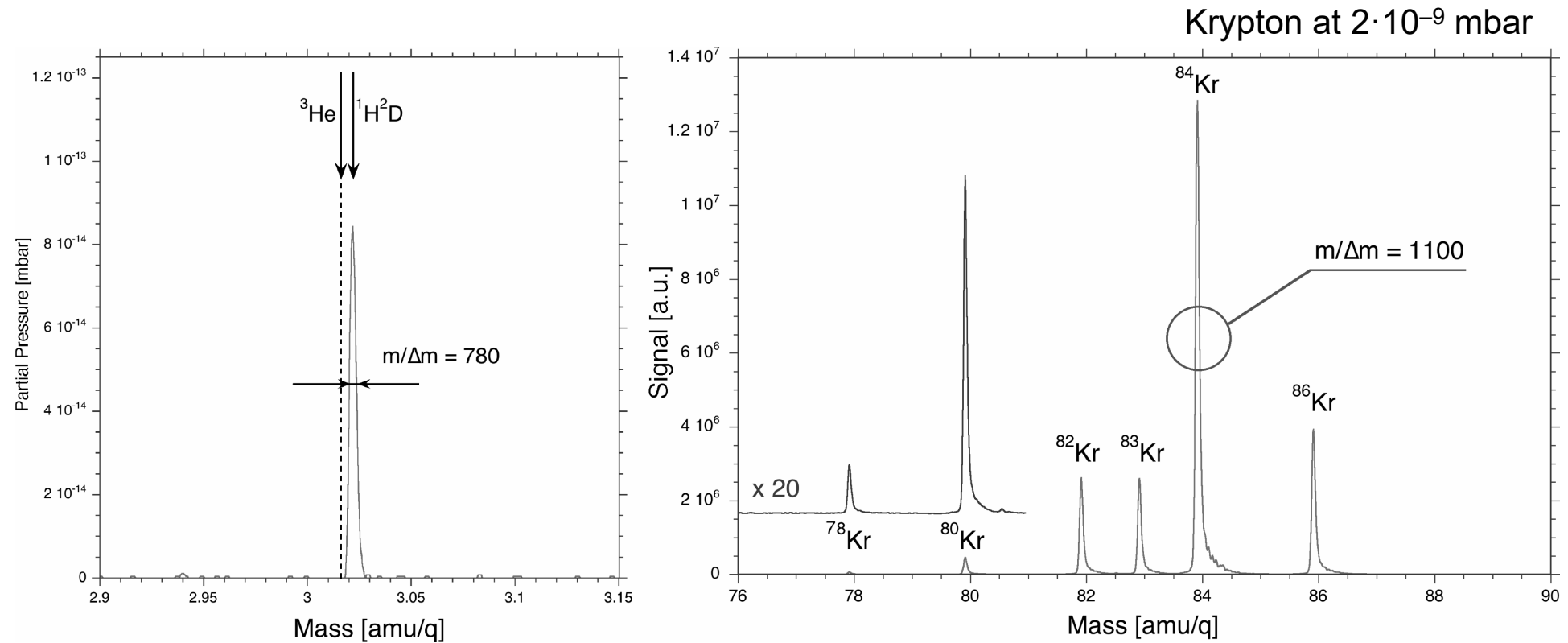


Mass spectrum acquired in th-mode, showing almost 5 decades of dynamic range with 8 bit ADC card



Prototype Results: Mass Resolution

PEP / NIM prototype

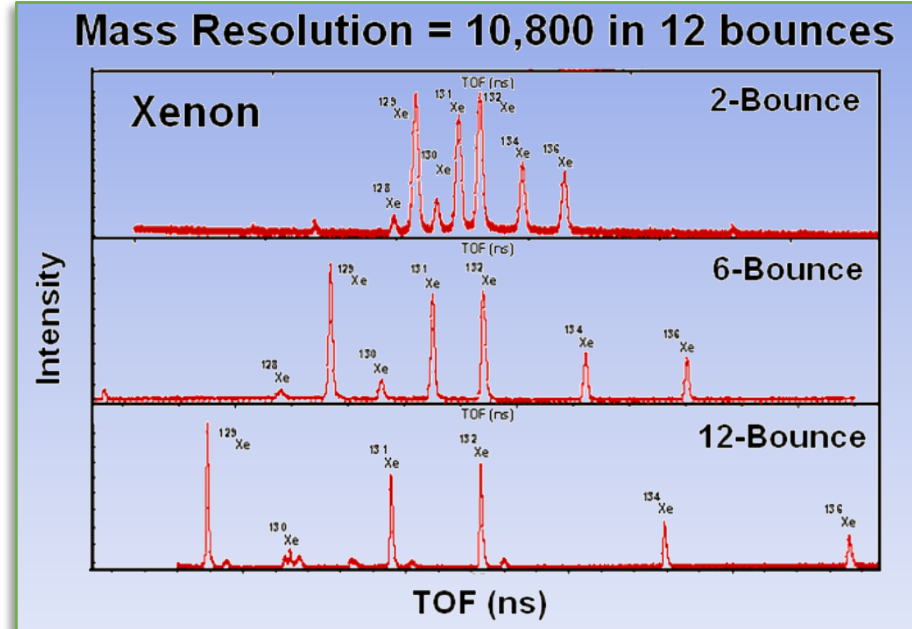
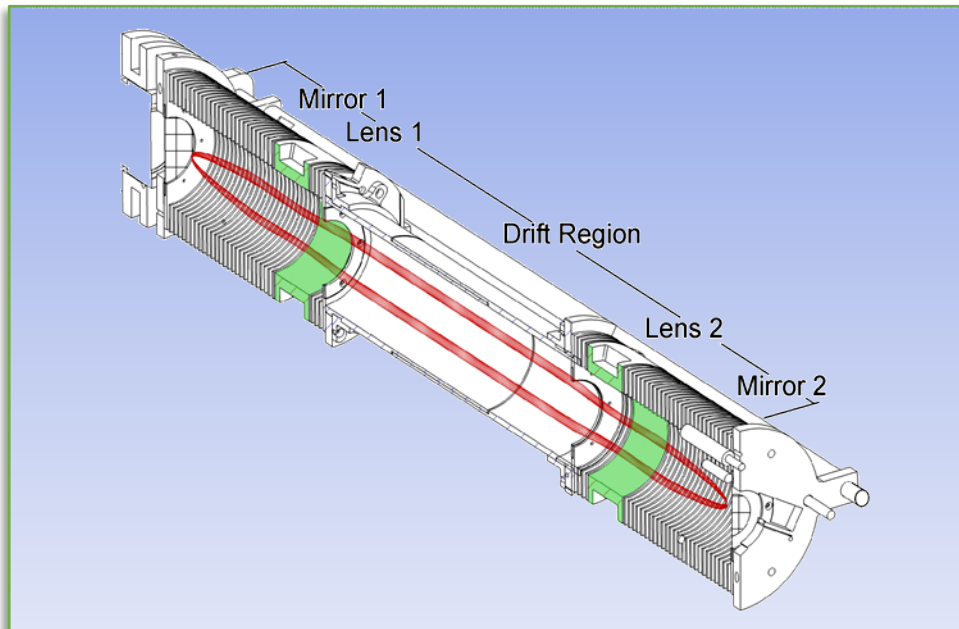
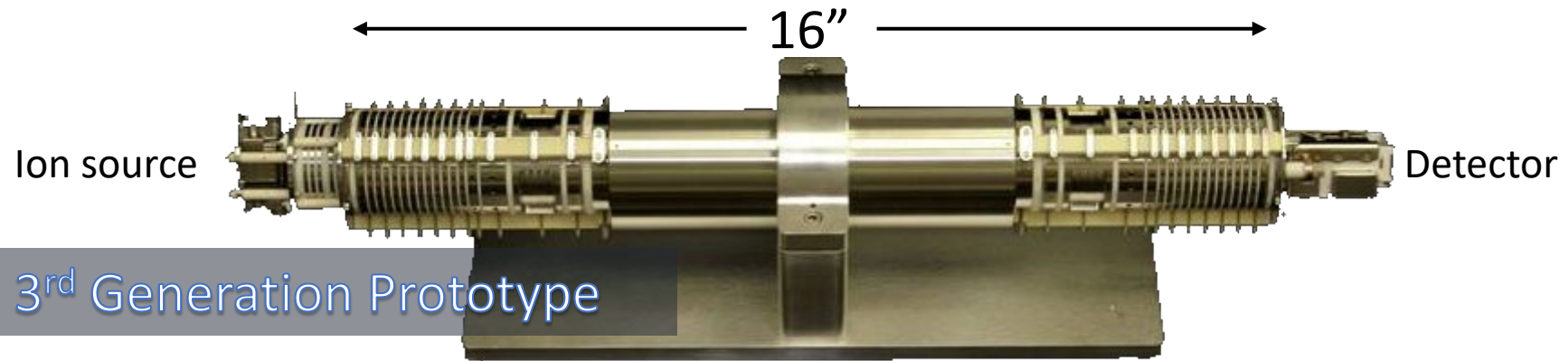


P. Wurz, D. Abplanalp, M. Tulej, and H. Lammer, Planet. Planet. Sp. Science 74 (2012) 264–269.

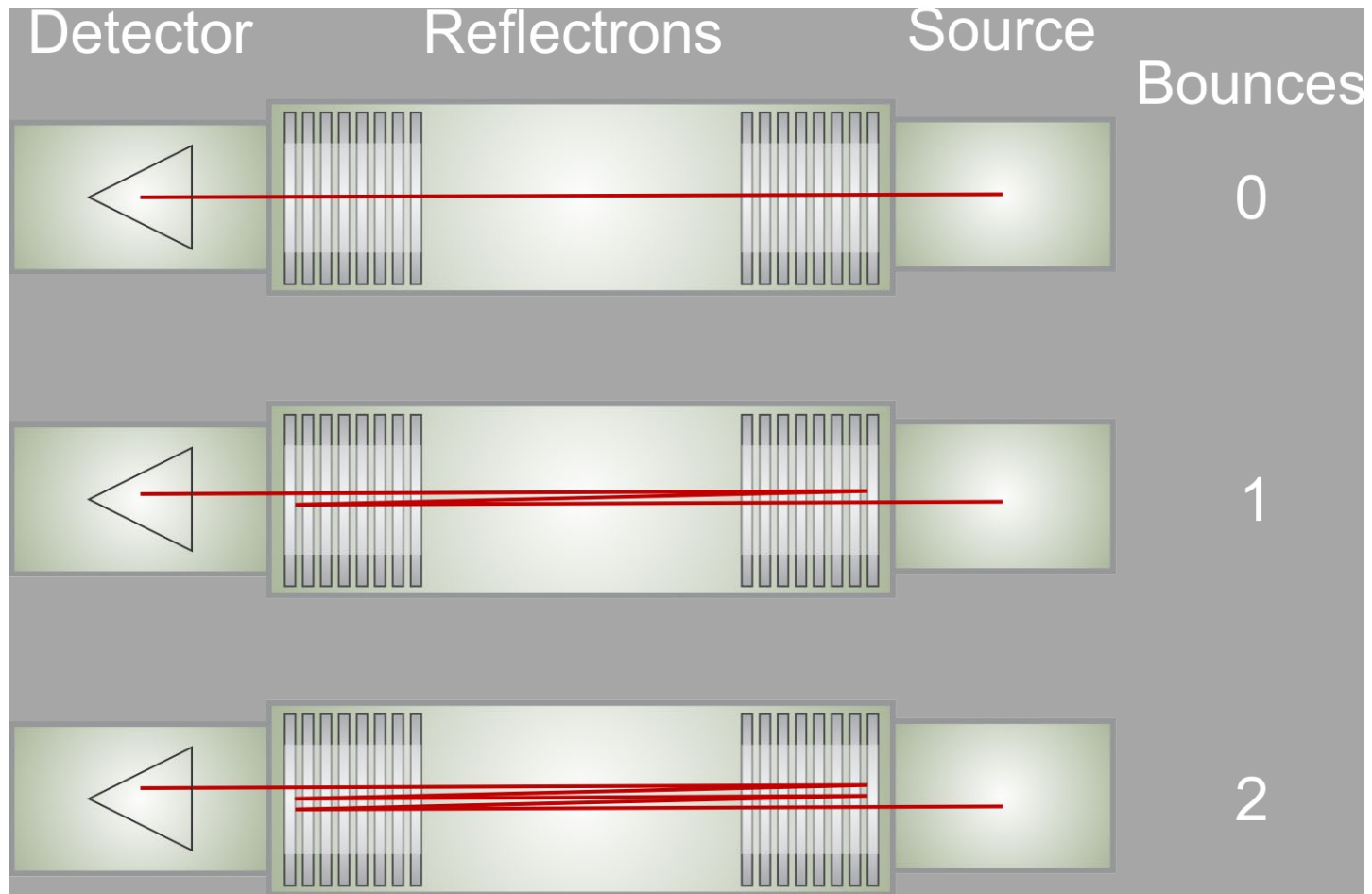
MASPEX: Unique Capabilities

- What uniquely enables MASPEX to accomplish these objectives?
 - A. Mass Resolution
 - B. Sensitivity

Resolution: Multi-Bounce Time-of-Flight

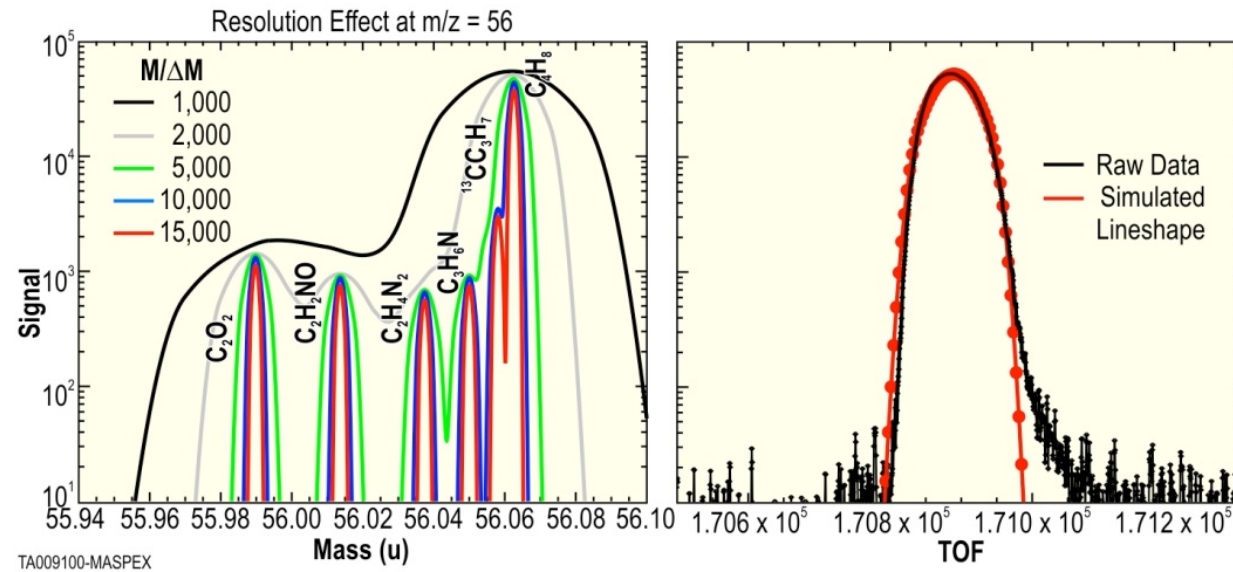


MBTOF principle

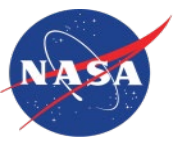


The Importance of Mass Resolution

Studies of the Enceladus plume hint at the presence of a large number of possible organic compounds whose identification is hindered by the low resolution of Cassini INMS. The simulation (left) demonstrates how increasing resolution enables the individual fragment ions (created by electron impact ionization within the source) of parent organic molecules to be fully separated and quantified. The spectrum (right) shows how the peak shape used in the simulation derived from MASPEX laboratory data.



A comprehensive simulation of the expected Europa environment was performed in the same way to identify the optimum analyte fragments and the resolution necessary for full separation. This information is used to define MASPEX's science operation modes.



Sensitivity



- Ion storage source

- 10^5 ions per extraction leading to.....

0.02 counts s^{-1} per molecule cm^{-3}

or

8×10^{-5} A per mbar @ 8×10^{-7} mbar source pressure

- Cryotrap

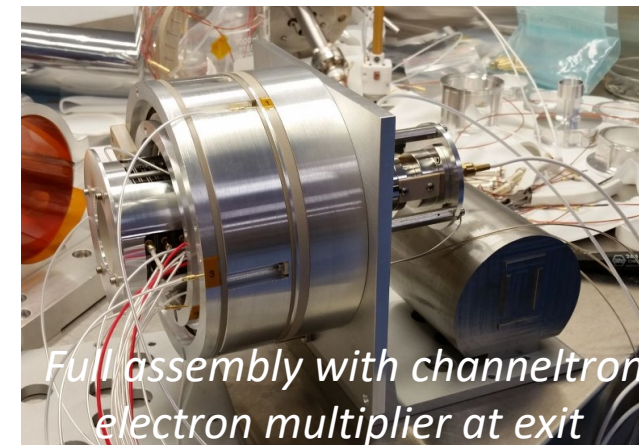
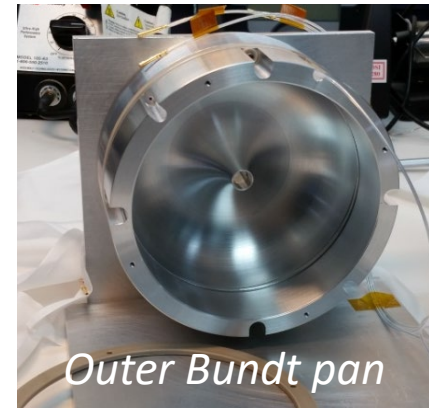
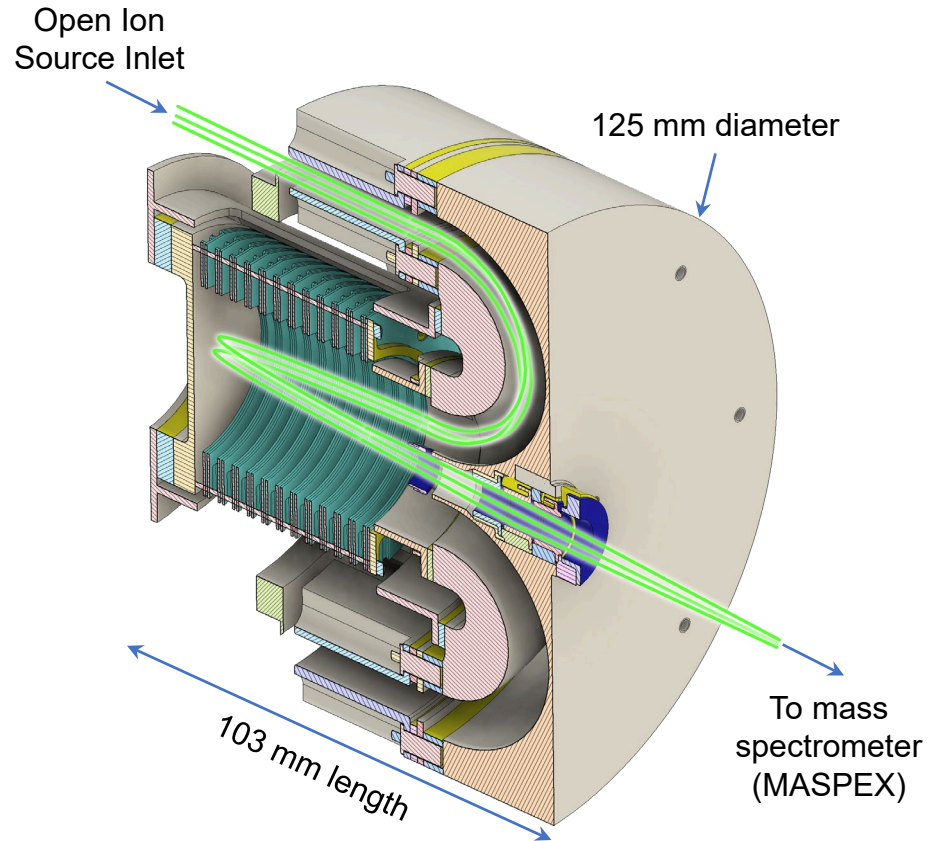
- Concentrates the sample to give an effective sensitivity of.....

RQ106.093 Closed Source Sensitivity

2000 counts s^{-1} per molecule cm^{-3}

High Performance Open Ion Source for Exploration (High-POISE)

A Bundt pan Electrostatic Analyzer (ESA) with reflectron for coaxial ion injection to mass spectrometers



Photographs of the prototype Bundt pan ESA open ion source.

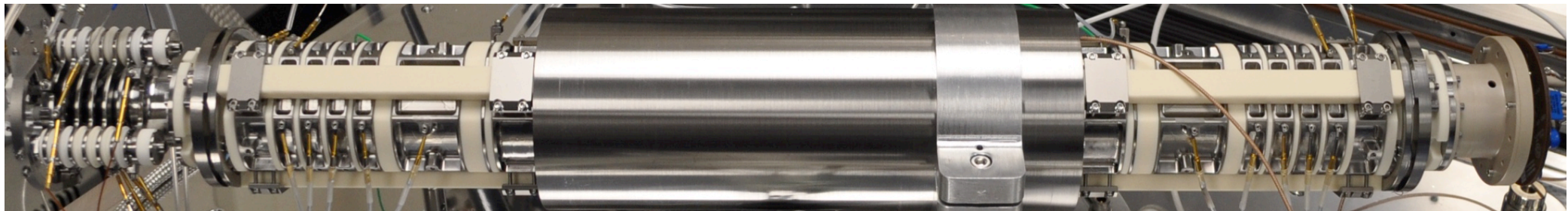
High-POISE enables:

- ✓ Increased accuracy in abundance measurements for neutrals and reactive neutrals versus closed ion source.
- ✓ Analysis of ions that are excluded (neutralized) in antechamber/gas inlet system of closed ion source.
- ✓ Analysis of larger molecular weight species (organics, amino acids, etc.) without worry of fragmentation
 - ✓ Debated that larger molecular weight species fragment in closed ion source systems due to their increased kinetic energy from space craft velocity
- ✓ Coaxial or orthogonal ion injection into a variety of mass spectrometers, including MASPEX (coaxial injection)

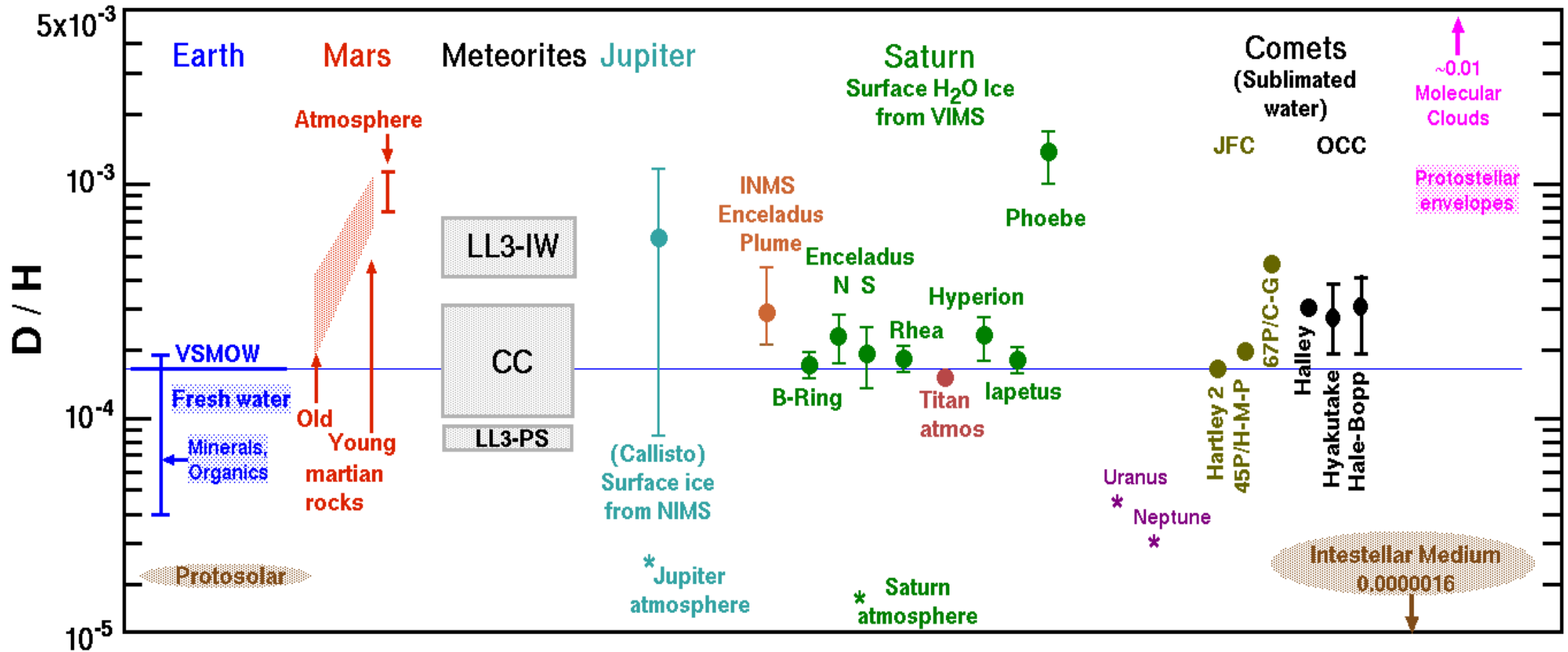
MASPEX-Europa



BACKUP SLIDES



D/H in Water measured to date



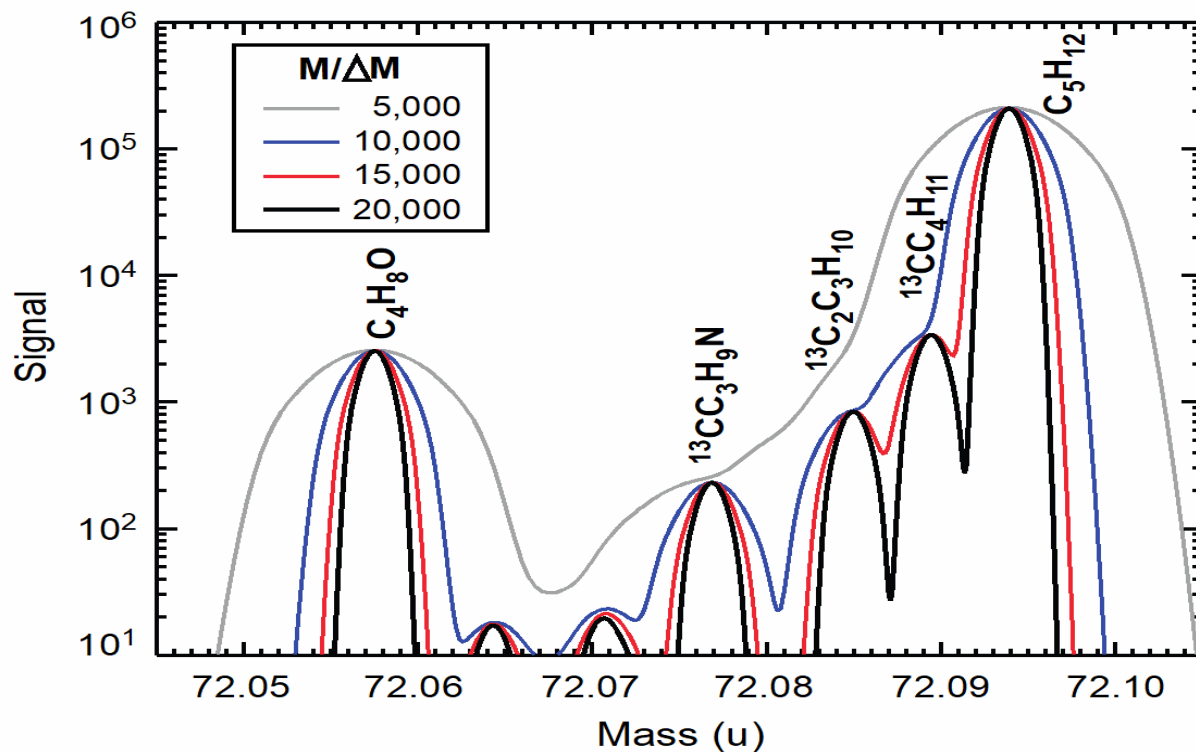
Measured D/H in the Solar System. Green symbols are Saturn System satellite (VIMS) and Callisto (NIMS) Clarke et al. (2018). Meteorites from Drake (2005), others as compiled by Hallis 2017 and referenced in Table 1. JFC= Jupiter family Comets. OCC= Ort Cloud Comets. Reference: **Isotopic Ratios of Saturn's Rings and Satellites: Implications for the Origin of Water and Phoebe**, Roger N. Clark, Robert H. Brown, Dale P. Cruikshank, and Gregg A. Swayze, accepted Icarus.

Mass resolution examples

- ${}^1\text{H}_2{}^{32}\text{S}$ versus ${}^{34}\text{S}$ requires ~ 1800 M/deltaM at 10% peak valley and the approximate abundance difference is 23.
- ${}^{34}\text{S}{}^{16}\text{O}_2$ versus ${}^{32}\text{S}{}^{18}\text{O}{}^{16}\text{O}$ requires ~ 8000 M/deltaM at 10% peak valley and the approximate abundance difference is 22.
- Organic molecules could further complicate this identification and they may arise from the ambient environment or spacecraft contamination.

Out-links (RPLRD)	ID	MASPEX ISPEC (L4 Spec)
When measuring the atmospheric composition dataset cryotrap samples, the mass resolution of MASPEX shall be $\geq 16,988$ as measured by the 10% valley definition between the Pentane C_5H_{12} and $^{12}C_4^{13}CH_{11}$ peaks. RQ104.719	RM-ISPEC-1230	The combination of all uncertainties in the MASPEX ion optics and detector system shall be less than the allowable error that enables the resolution requirement ($m/\delta m$) of 16,988 as measured by the 10% valley definition between the Pentane C_5H_{12} and $^{12}C_4^{13}CH_{11}$ peaks.

Resolution Effect at $m/z = 72$



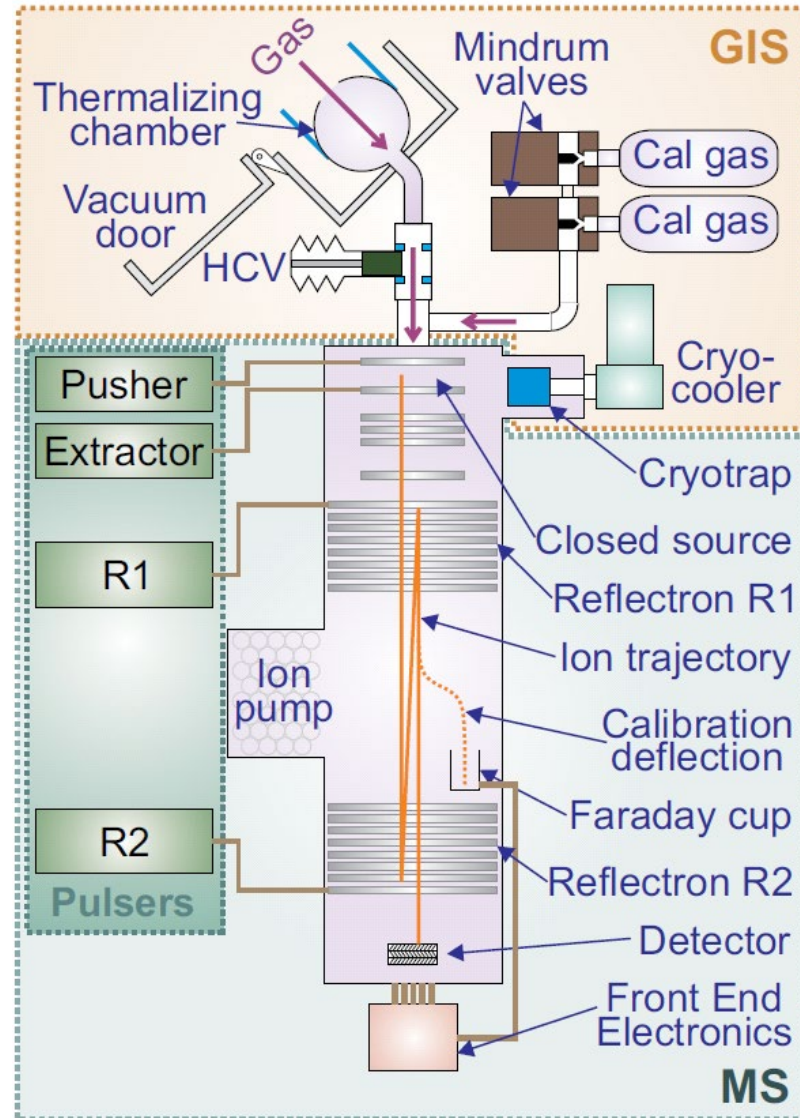
Simulations of the required measurements identify the key and driving requirements for the mass resolution.

Instrument Block Diagram

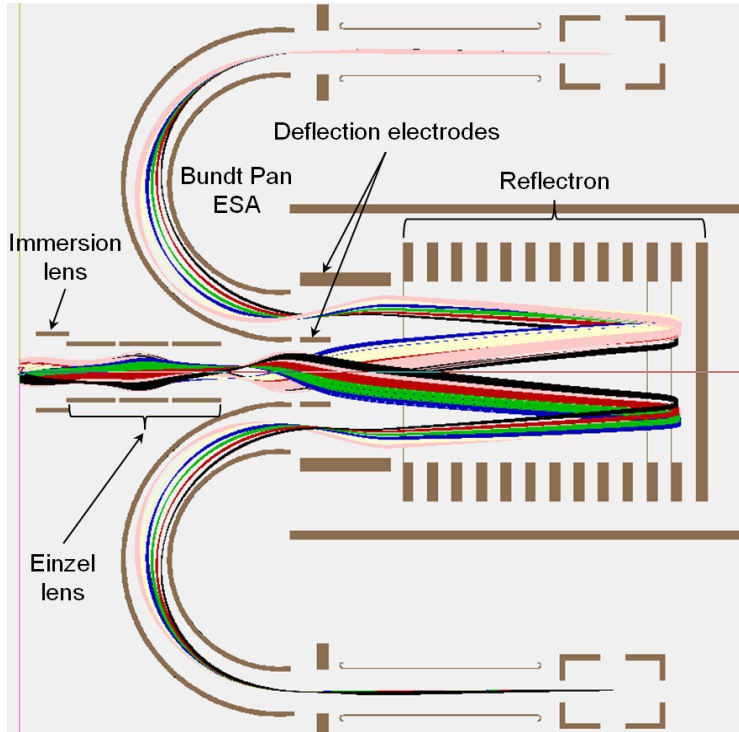
A block diagram of the instrument showing the major subsystems:

Gas inlet system (GIS)

Mass spectrometer (MS).

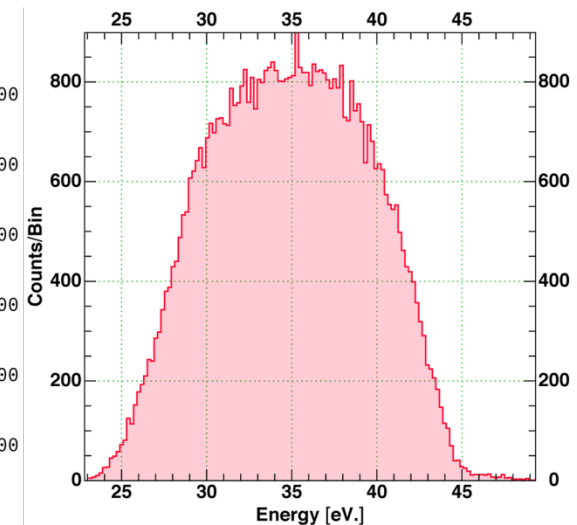
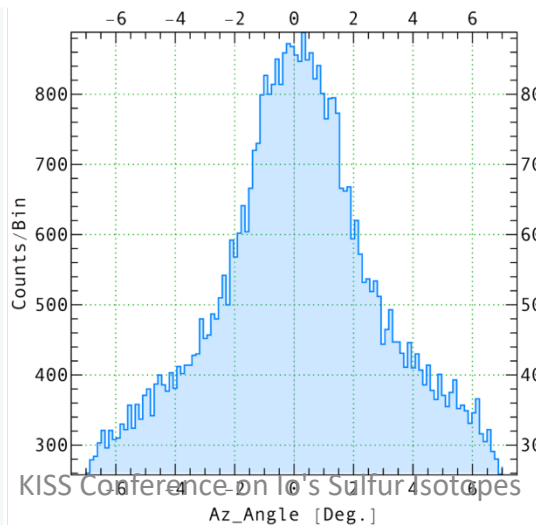
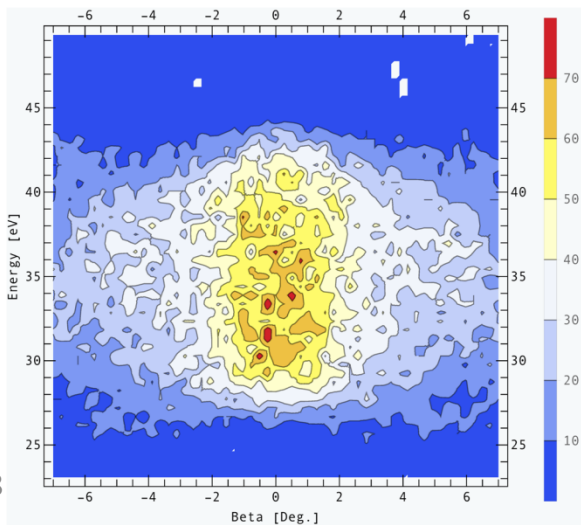


High Performance Open Ion Source for Exploration (High-POISE) – more info

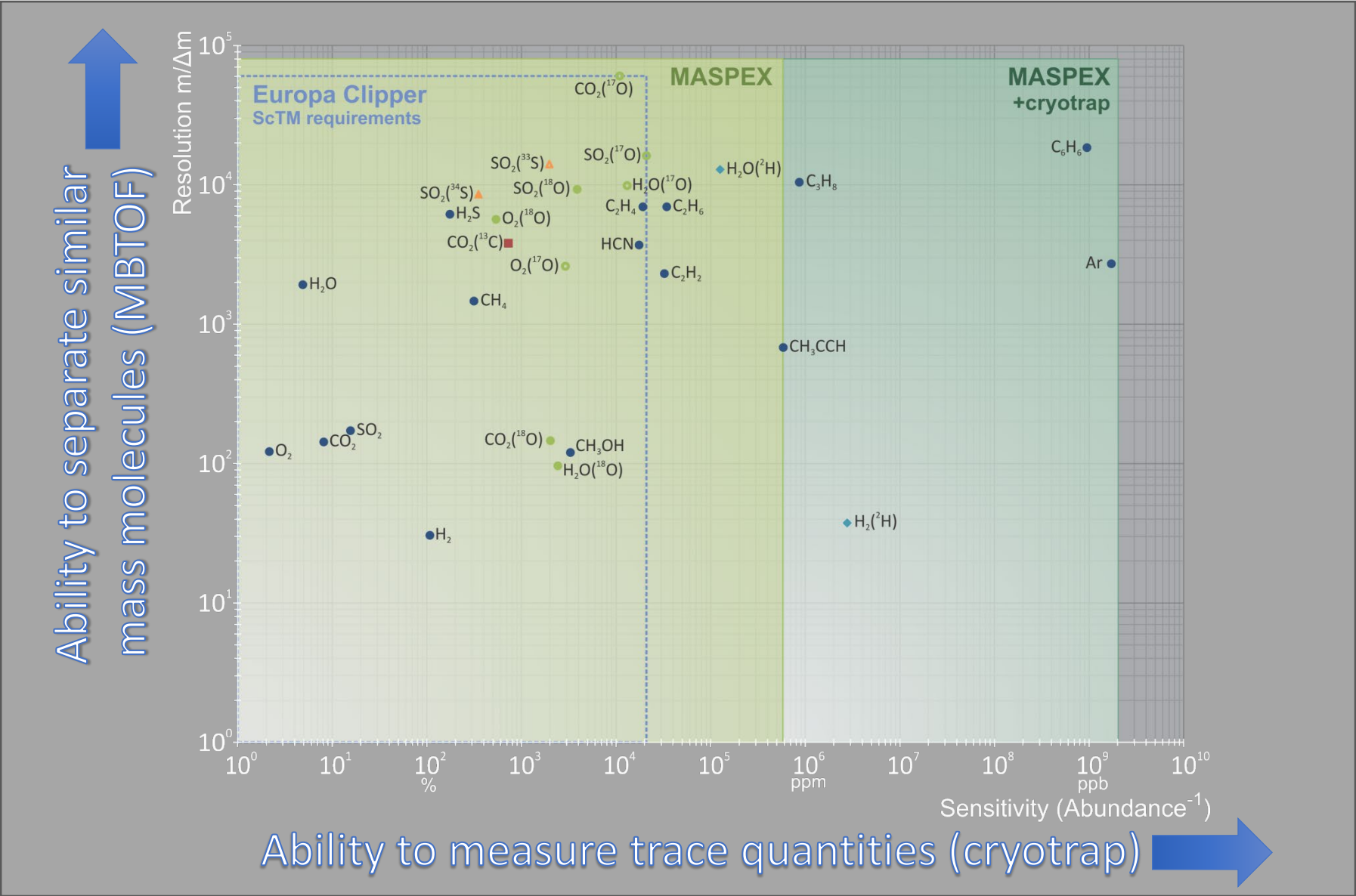


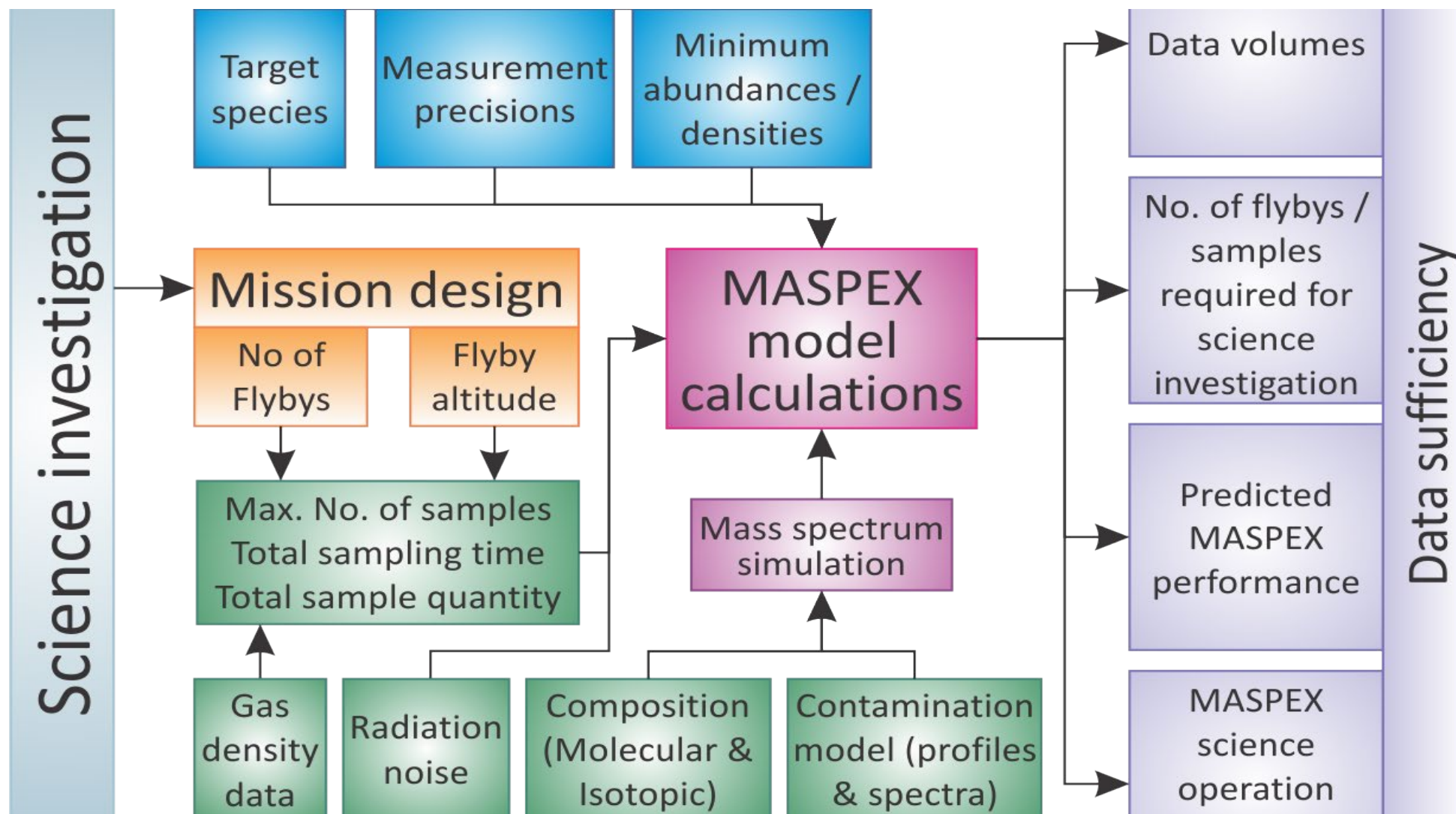
SIMION ray trace showing ion transmission through the entire device (top left).

SIMION simulation results displaying the Weene plot (bottom left), counts/bin versus azimuthal angle (angular resolution), and counts/bin versus energy (energy resolution) of the device.



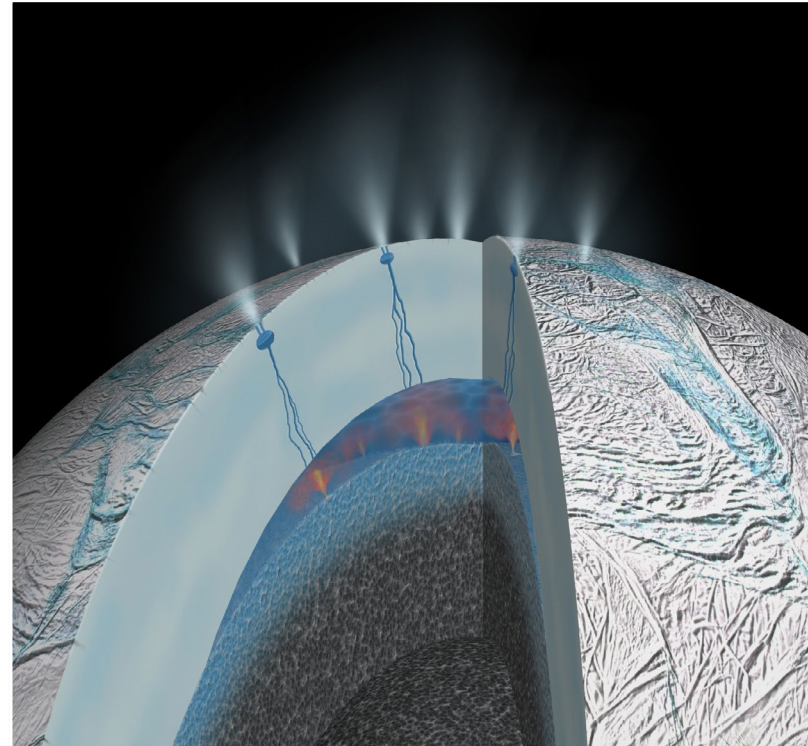
MASPEX Performance





COSMIC DUST ANALYZER

- Analysis of salty ice grains in the plume (Postberg et al., Nature 2009 & 2011)
 - Presence of an ocean plume-source & ocean in contact with rock
- Constrained ocean salinity and alkaline pH:
 - $\text{NaCl} \sim 0.5 - 1\%$, $\text{NaHCO}_3 \sim 0.2 - 0.5\%$, and $\sim 8.5 - 9$
- Detection of nano-phase silica emitted by Enceladus (Hsu et al., Nature 2015)
 - Presence of alkaline hydrothermal systems ($T \geq 90^\circ\text{C}$)
 - Fast transport of material from core to plume





The Neutral Gas and Ion Mass Spectrometer of the PEP Experiment on the JUICE Mission

Peter Wurz, Stefan Meyer, André Galli, Marek Tulej, Audrey Vorburger,
Davide Lasi, Daniele Piazza, and Matthias Lüthi

Physikalisches Institut, Universität Bern, 3012 Bern, Switzerland

Pontus Brandt

The Johns Hopkins University, Applied Physics Laboratory, Laurel, MD, USA

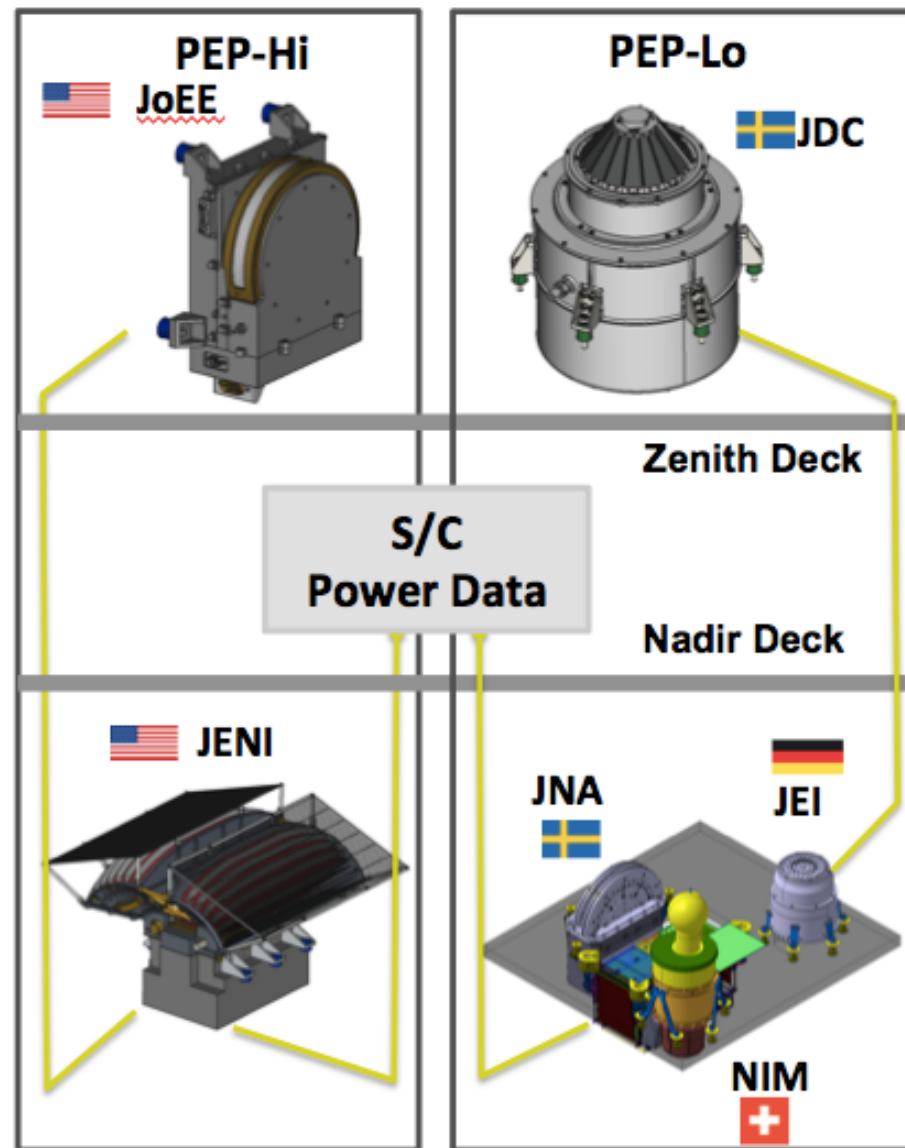
Stas Barabash

Swedish Institute of Space Physics, S-981 28 Kiruna, Sweden



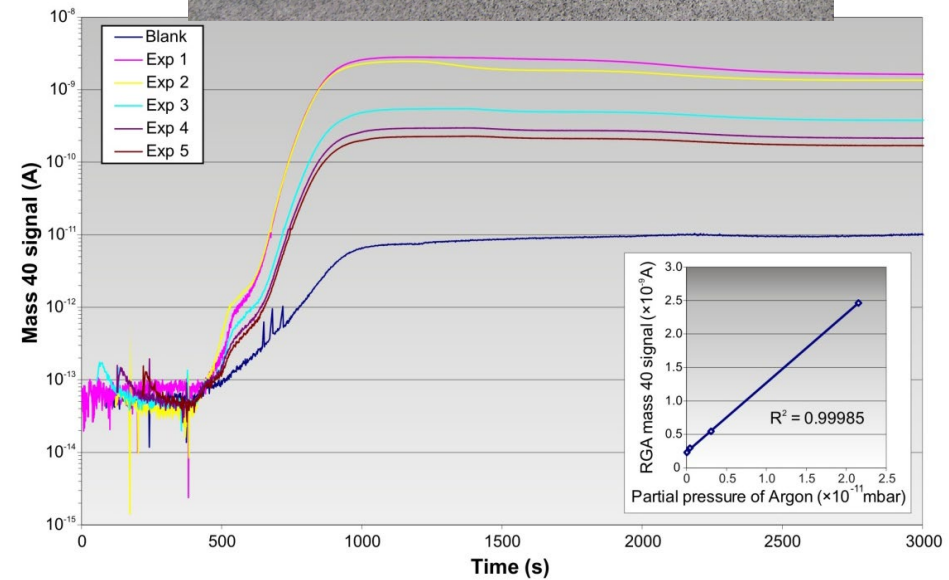
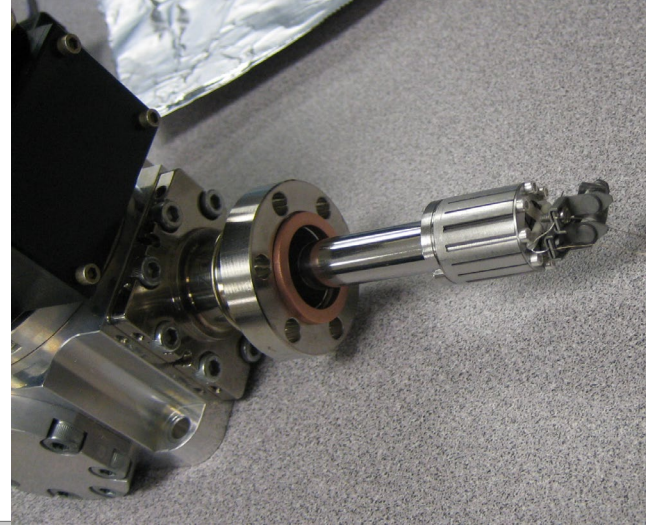
Particle Environment Package (PEP) Instrument

- PEP includes 6 sensors
 - JDC: Ion spectrometer and mass analyzer (electron capabilities)
 - JEI: Electron spectrometer (ion capabilities)
 - JoEE: Energetic electrons spectrometer
 - JENI: Energetic ion spectrometer and ENA imager (electron capabilities)
 - JNA: Low energy ENA imager
 - NIM: Neutral gas and ion mass spectrometer
- Seven mechanical units arranged in two groups **PEP-Lo** and **PEP-Hi**, located on the nadir and zenith plane of the spacecraft

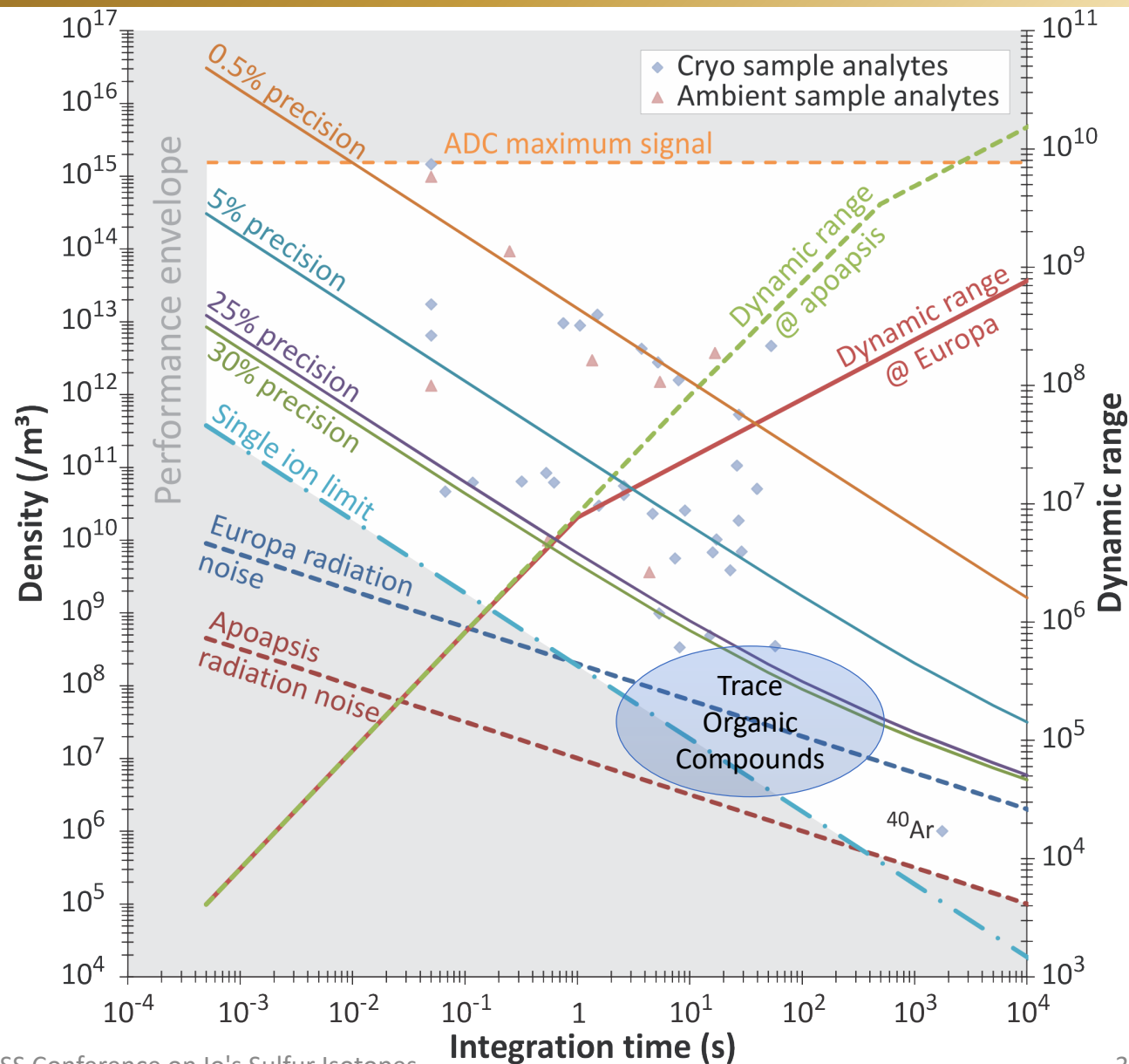


Sensitivity: Cryo-trapping

- Flight heritage Ricor cryocooler
- Sintered 316L SS absorber
- Quantitative absorption and release of Argon
- Increases sensitivity by a factor of >10,000



Ambient analytes that fall below the radiation noise line or require integration in excess of a single flyby must be measured by cryotrapping



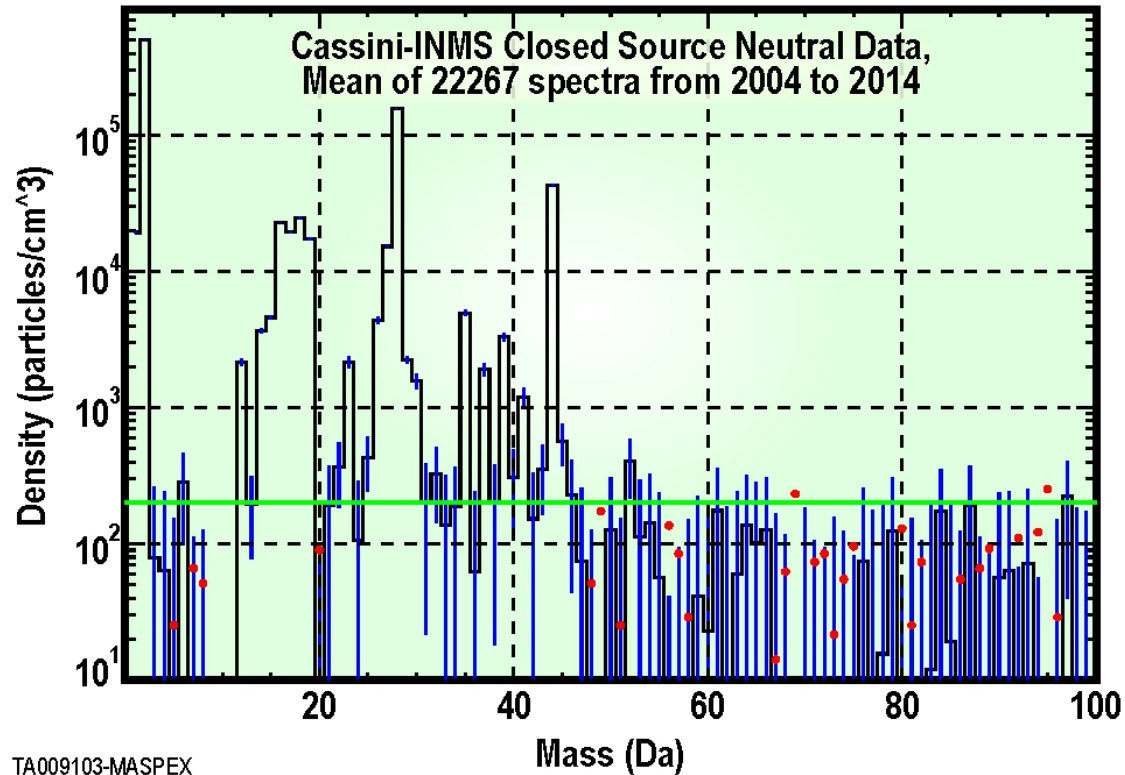
Contamination Control

- Why is contamination control so important?

Origins of SMOG

- Desorption
 - All surfaces have a covering of physisorbed material that will outgas
- Decomposition
 - Breakdown of solids to produce more volatile molecules
- Diffusion
 - Gas dissolved in solids diffuses to the surface
- Permeation
 - Trapped gas permeates through solids to the surface
- Thrusters
 - Designed to 'outgas' material rapidly

Cassini INMS SMOG



The green horizontal line is the limit of detection of Cassini INMS as determined from the dark counts in mass channels where no signal is observed and attributed to radiation and cosmic rays.

The data is derived from the majority of Titan flybys, inbound between CA-3500 sec and CA-950 seconds.